Insect Biochemistry and Molecular Biology 122 (2020) 103392

Contents lists available at ScienceDirect

Insect Biochemistry and Molecular Biology

journal homepage: www.elsevier.com/locate/ibmb

Can BRET-based biosensors be used to characterize G-protein mediated signaling pathways of an insect GPCR, the *Schistocerca gregaria* CRF-related diuretic hormone receptor?

Els Lismont[a,1], Lina Verbakel[a,*,1], Elise Vogel[a], Jenny Corbisier[b], Gaetan-Nagim Degroot[b], Rik Verdonck[a], Heleen Verlinden[a], Elisabeth Marchal[a,b], Jean-Yves Springael[c], Jozef Vanden Broeck[a]

[a] *Molecular Developmental Physiology and Signal Transduction, KU Leuven, Naamsestraat 59, P.O. Box 02465, B-3000, Leuven, Belgium*
[b] *Imec, Kapeldreef 75, B-3001, Leuven, Belgium*
[c] *Institut de Recherche Interdisciplinaire en Biologie Humaine et Moléculaire (IRIBHM) Université Libre de Bruxelles (ULB), Campus Erasme, 808 Route de Lennik, B-1070, Brussels, Belgium*

ARTICLE INFO

Keywords:
BRET
Cyclic AMP
G protein-coupled receptor
Insect
Neuropeptide
Reporter assay

ABSTRACT

G protein-coupled receptors (GPCRs) are membrane-bound receptors that are considered prime candidates for the development of novel insect pest management strategies. However, the molecular signaling properties of insect GPCRs remain poorly understood. In fact, most studies on insect GPCR signaling are limited to analysis of fluctuations in the secondary messenger molecules calcium (Ca^{2+}) and/or cyclic adenosine monophosphate (cAMP). In the current study, we characterized a corticotropin-releasing factor-related diuretic hormone (CRF-DH) receptor of the desert locust, *Schistocerca gregaria*. This *Schgr*-CRF-DHR is mainly expressed in the nervous system and in brain-associated endocrine organs. The neuropeptide *Schgr*-CRF-DH induced Ca^{2+}-dependent aequorin-based bioluminescent responses in CHO cells co-expressing this receptor with the promiscuous $G\alpha_{16}$ protein. Furthermore, when co-expressed with the cAMP-dependent bioluminescence resonance energy transfer (BRET)-based CAMYEL biosensor in HEK293T cells, this receptor elicited dose-dependent agonist-induced responses with an EC_{50} in the nanomolar range (4.02 nM). In addition, we tested if vertebrate BRET-based G protein biosensors, can also be used to detect direct Gα protein subunit activation by an insect GPCR. Therefore, we analyzed ten different human BRET-based G protein biosensors, representing members of all four Gα protein subfamilies; $G\alpha_s$, $G\alpha_{i/o}$, $G\alpha_{q/11}$ and $G\alpha_{12/13}$. Our data demonstrate that stimulation of *Schgr*-CRF-DHR by *Schgr*-CRF-DH can dose-dependently activate $G\alpha_{i/o}$ and $G\alpha_s$ biosensors, while no significant effects were observed with the $G\alpha_{q/11}$ and $G\alpha_{12/13}$ biosensors. Our study paves the way for future biosensor-based studies to analyze the signaling properties of insect GPCRs in both fundamental science and applied research contexts.

1. Introduction

Neuropeptides regulate key biological processes, such as development, growth, metabolism, ecdysis, feeding, and reproduction, in a very precise and controlled manner. The majority of neuropeptides signal through G protein-coupled receptors (GPCRs), membrane-bound receptors which are often regarded as candidate targets for novel insect pest management strategies (Gäde and Goldsworthy, 2003; Verlinden et al., 2014). The GPCR superfamily has been studied extensively in vertebrates, since these receptors are pharmacological targets for many important therapeutic compounds (Pierce et al., 2002). In insects, however, the molecular signaling properties of GPCRs remain poorly understood. Fortunately, numerous *in vitro* assays have been developed to study the GPCR signaling cascades. Most of these assays focus on fluctuations in downstream intracellular secondary messenger levels, such as Ca^{2+} and cyclic AMP (cAMP). For instance, an aequorin bioluminescence assay is frequently utilized to monitor possible changes in intracellular Ca^{2+} levels. Similarly, a cAMP response element (CRE) dependent luciferase reporter assay, using a $CRE_{(6x)}$-Luc construct, enables the monitoring of variations in intracellular cAMP levels. Both

* Corresponding author.
E-mail address: lina.verbakel@kuleuven.be (L. Verbakel).
[1] These authors contributed equally to this manuscript.

https://doi.org/10.1016/j.ibmb.2020.103392
Received 27 November 2019; Received in revised form 1 April 2020; Accepted 19 April 2020
Available online 05 May 2020
0965-1748/

assays and the cell lines used in these assays have proven their value in insect GPCR characterization studies (Bil et al., 2016; Caers et al., 2016a, 2016b; Dillen et al., 2013; Horodyski et al., 2011; Huang et al., 2014; Lenaerts et al., 2017; Lismont et al., 2015, 2018; Marchal et al., 2018; Meeusen et al., 2002; Mertens et al., 2002; Poels et al., 2007, 2009; 2010; Vandersmissen et al., 2013; Verlinden et al., 2013, 2015; Vleugels et al., 2013; Vuerinckx et al., 2011; Zels et al., 2014). However, the bioluminescence measured using the $CRE_{(6x)}$-Luc construct is not directly induced by cAMP but is dependent on the phosphorylation of the CRE binding protein (CREB). As there is some speculation that CREB can also be phosphorylated by calcium/calmodulin-dependent protein kinase, bioluminescence measured in this way may also be caused by increased Ca^{2+} levels (Johannessen et al., 2004). Therefore, several alternative methods have been developed to monitor changes in intracellular cAMP levels in cell based GPCR assays. The bioluminescence resonance energy transfer ($BRET^1$)-based assay, using YFP-Epac-*R*luc (CAMYEL) as a biosensor for cAMP (ATCC MBA-277), is such an alternative method. Using this biosensor, decreasing or increasing levels of intracellular cAMP upon GPCR activation are monitored by an increase or a decrease in $BRET^1$signal, respectively (Jiang et al., 2007L). A schematic representation of this CAMYEL biosensor-based cAMP reporter assay (adapted from Matthiesen and Nielsen, 2011) is presented in Fig. 1A. This assay was developed to study the biology, pharmacology and signaling of GPCRs that regulate the adenylyl cyclase (AC)/cAMP pathway (Jiang et al., 2007). However, by only monitoring fluctuations in second messenger levels, we cannot precisely infer which specific Gα protein(s) is (are) activated upon receptor activation. Therefore, to further study vertebrate G protein mediated signaling pathways, $BRET^2$-based G protein biosensors were developed to detect direct activation of the Gα subunit after GPCR activation. To study their coupling with mammalian GPCRs, ten different human G protein-based biosensors representing all four Gα protein subfamilies ($G\alpha_{i/o}$, $G\alpha_s$, $G\alpha_{q/11}$ and $G\alpha_{12/13}$) have been validated. Each individual biosensor consists of three constructs, Gα-Rluc8, $G\beta_1$ and $G\gamma_2$-GFP10, which form a $\alpha_x\beta_1\gamma_2$ G protein heterotrimer, with α_x representing one of ten different Gα subunit constructs. These biosensors enable the real-time detection of Gα activation upon receptor stimulation (Denis et al., 2012; Galés et al., 2006) while simultaneously verifying which particular member of this family is activated (Galés et al., 2006). A schematic representation of this assay (adapted from Galés et al., 2006) is depicted in Fig. 1B. While this assay has proven its value in the study of the G protein-mediated signaling pathways of several vertebrate GPCRs (Audet et al., 2008; Bellot et al., 2015; Bruzzone et al., 2014; Busnelli et al., 2012; Capra et al., 2013; Corbisier et al., 2015; Damian et al., 2015; De Henau et al., 2016; Galandrin et al., 2008, 2016; Galés et al., 2006; Garcia et al., 2018; Hansen et al., 2013; Leduc et al., 2009; Maurice et al., 2010; Peverelli et al., 2013; Rives et al., 2012 Onfroy et al., 2017; Saulière et al., 2012; Schmitz et al., 2014; Schrage et al., 2015), to our knowledge, it has never been employed to analyze G protein-mediated signaling pathways of insect GPCRs, despite the fact that insect GPCRs are typically characterized by heterologous expression in mammalian cell lines.

In the current study, we therefore verified the application of BRET-based assays for insect GPCR research. For this purpose, we identified and characterized a corticotropin-releasing factor (CRF)-related diuretic hormone (DH) receptor from the desert locust *Schistocerca gregaria*, an insect known for its extreme form of density dependent polyphenism (Cullen et al., 2017). The role of its ligand, CRF-DH, has been well established as a diuresis stimulator in the excretory system of various insects (Cannell et al., 2016; Coast and Kay, 1994; Furuya et al., 2000; Te Brugge et al., 2011). Besides its diuresis activating properties, CRF-DH is suggested to induce satiety in *S. gregaria*, *Locusta migratoria,* and *Rhodnius prolixus* (Van Wielendaele et al., 2012; Audsley et al., 1997; Goldsworthy et al., 2003; Lee et al., 2016; Mollayeva et al., 2018). In addition, CFR-DH initiates pre-ecdysis in *Manduca sexta* (Kim et al., 2006), regulates sperm retention and storage in the spermatheca in *Drosophila melanogaster* (Lee et al., 2015) and retards oocyte growth in *S. gregaria* (Van Wielendaele et al., 2012).

While the physiological role of *Schgr*-DH was previously investigated in *S. gregaria* (Van Wielendaele et al., 2012), its receptor was never molecularly characterized. Moreover, this newly characterized receptor, *Schgr*-CFR-DHR, was also chosen as a proof-of-principle, since it is well-documented that CRF-DHs exert effects on their cellular targets through their interaction with receptors belonging to the secretin receptor-related GPCR family (family B), for which cAMP has been identified to act as an intracellular second messenger of CRF-DH in numerous insects, both *in vivo* and *in vitro* (Audsley et al., 1995; Baldwin et al., 2001; Clottens et al., 1994; Hector et al., 2009; Johnson

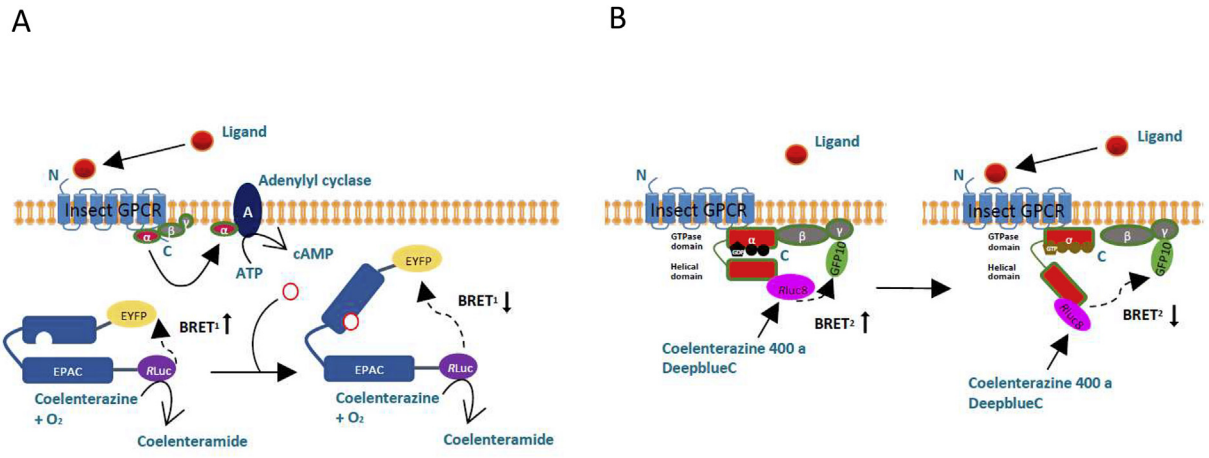

Fig. 1. Schematic representation of both BRET1 and BRET2 systems. A) Schematic representation of the cAMP reporter assay using the CAMYEL biosensor: the protein exchange factor directly activated by cAMP (EPAC) is flanked by yellow fluorescent protein (YFP) and Rluc. Upon binding of cAMP to EPAC, a conformational change is induced which results in a larger distance between YFP and Rluc. As a consequence, bioluminescence energy transfer ($BRET)^1$ decreases. Coelenterazine acts as a substrate for Rluc (Image adapted from Matthiesen and Nielsen, 2011). B) Schematic representation of the $BRET^2$-based G protein biosensors. The energy donor, *R*luc8, is genetically coupled into the helical domain of Gα. GFP10 is N-terminally linked to Gγ. In resting state, when the G protein-coupled receptor (GPCR) is not stimulated by a ligand, the donor *R*luc8 and the acceptor GFP10 are in proximity, inducing a high $BRET^2$ signal. Upon binding of the ligand to the receptor, this GPCR is activated, inducing the activation of the Gα subunit. When the Gα subunit is activated, GDP is exchanged for GTP and a large interdomain movement in Gα is induced resulting in a larger distance between the donor *R*luc8 and the acceptor GFP10, consequently leading to a lower $BRET^2$ signal (Image adapted from Bellot et al., 2015). (For interpretation of the references to color in this figure legend, the reader is referred to the Web version of this article.)

et al., 2004; Lee et al., 2016; Reagan, 1996; Tobe et al., 2005). In addition, the production of primary urine is dependent on cAMP, which increases cationic transport (such as K^+ and Na^+) into the Malpighian tubules (Beyenbach, 1995; O'Donnell et al., 1996). The first insect CRF-DH receptor (CRF-DHR) was characterized *in vitro* in *M. sexta* (Reagan, 1995), followed by *in vitro* characterizations of additional homologues in following species; *Acheta domesticus* (Reagan, 1996), *R. prolixus* (Lee et al., 2016) and *D. melanogaster* (Hector et al., 2009; Johnson et al., 2004).

In the present study, *Schgr*-CRF-DHR was cloned from a desert locust brain cDNA library. Quantitative real-time PCR (qRT-PCR) revealed spatial expression patterns of *Schgr*-CRF-DHR in tissues derived from the locust central nervous system. We have further characterized this receptor in cell-based functional receptor assays: downstream signaling effects were studied by means of the aequorin bioluminescence assay and the BRET[1]-based CAMYEL (ATCC MBA-277) biosensor. Furthermore, direct activation of G-proteins was measured using the BRET[2]-based biosensors (Galés et al., 2006).

2. Materials and methods

2.1. Sequence analysis of Schgr-CRF-DHR

The nucleotide sequence of a putative CRF-DH receptor (*Schgr*-CRF-DHR) was identified by means of a local BLAST scan of a brain-specific transcriptome database of gregarious *S. gregaria* created by illumina-sequenced reads (unpublished data). As depicted below, amino acid sequences of the putative *Schgr*-CRF-DHR were compared with amino acid sequences of other insect CRF-DHRs that have been characterized *in vitro*: *D. melanogaster* (*Drome*-DH44-R1; *GenBank: NP_610960.1*, and *Drome*-DH44-R2; *GenBank: NP_610789.3*), *R. prolixus* (*Rhopr*-CRF-DHR2B; *GenBank: KJ407397*), *M. sexta* (*Manse*-CRF-DHR; *GenBank: AAC46469.1*) and *A. domesticus* (*Achdo*-CRF-DHR; *GenBank: AAC47000.1*).

A multiple sequence alignment and a percent identity matrix were constructed by using the EMB-EBI Clustal Omega Multiple Sequence alignment software (http://www.ebi.ac.uk/Tools/msa/clustalo/). Conservation of the amino acids was predicted using MEGA 7. Figures were created using T-COFFEE Multiple sequence alignment server (http://tcoffee.crg.cat/apps/tcoffee/do:mcoffee) and the BOXSHADE 3.21 server (http://www.ch.embnet.org/software/BOX_form.html). Putative transmembrane regions (TM1-TM7) were predicted by the TMHMM Server v. 2.0 (http://www.cbs.dtu.dk/services/TMHMM/). An additional percent identity matrix was created using receptor sequences from TM1 to TM7 using the EMB-EBI Clustal Omega Multiple Sequence alignment software.

2.2. Rearing of animals and tissue collection

S. gregaria was reared under crowded conditions (> 200 locusts/cage) as described by Lismont et al. (2015). In the reported experiments, multiple tissues were collected from both immature and mature gregarious locusts of both sexes, as CRF-DH plays a role in reproduction of this locust species (Van Wielendaele et al., 2012). The locusts were synchronized on the day of adult ecdysis and placed in separate cages. Immature males and females were dissected on day three after their molt into adults. The locust tissues and organs of interest were dissected under a binocular microscope and rinsed in locust Ringer solution (1L: 8.766 g NaCl; 0.188 g CaCl2; 0.746 g KCl; 0.407 g MgCl2; 0.336 g NaHCO3; 30.807 g sucrose; 1.892 g trehalose). In this way, brain, optic lobes, ventral nerve cord, gonads, fat body, flight muscle, foregut, caeca, Malpighian tubules, midgut, hindgut, male accessory glands, as well as a piece of the epidermis with its cuticle, were removed and collected in 2.0 mL tubes containing MagNa Lyser green beads (Roche). Additionally, the corpora cardiaca, corpora allata, the prothoracic gland, the frontal ganglion, and the suboesophageal ganglion were collected in RNase-free Screw Cap Micro centrifuge tubes. The same tissues were collected for the samples taken from mature insects. Mature males were dissected 12–13 days after molting, when they had a yellow cuticle coloration, an indication of gregarious male maturity. Mature females were similarly dissected 10–13 days after molting, but only if they were in the vitellogenic stage of ovarian maturation. During this stage, the oocyte size strongly increases from 1.7 to 7 mm and oocytes start showing a yellow color (Tobe and Pratt, 1975). For this study, tissues were only collected from females with oocyte sizes ranging from 3 to 6 mm. For every tissue or organ in each condition, four pools were dissected consisting of eight animals each. All samples were immediately snap frozen in liquid nitrogen to prevent RNA degradation. Until further processing, the samples were stored at −80 °C.

2.3. RNA extraction and cDNA synthesis

Depending on the tissue, different RNA extraction methods were used. RNA extractions of the tissues collected in the MagNa Lyser green beads tubes were performed utilizing the RNeasy Lipid Tissue Mini Kit (Qiagen, Germantown, MD), according to the manufacturer's protocol. A DNase treatment (RNase-Free DNase set, Qiagen) was performed to eliminate potential genomic DNA contamination. Because of their relatively small size, RNA extractions of the tissues collected in the RNase-free Screw Cap Microcentrifuge tubes were executed using the RNAqueous-Micro Kit (Ambion) according to the manufacturer's instructions. The recommended DNase step was subsequently performed. RNA quantity and quality were verified using a Nanodrop spectrophotometer (Thermo Fisher Scientific Inc.). cDNA of all samples was synthesized using the PrimeScript RT reagent Kit (Perfect Real Time) from TaKaRa, according to the manufacturer's instructions. The resulting cDNA was diluted tenfold.

2.4. Quantitative real-time PCR (qPCR)

All primers used for qPCR profiling are presented in Supplementary Table S1. All qPCR reactions were performed in duplicate in 96-well plates on a StepOne System (ABI Prism, Applied Biosystems), as described by Lenaerts et al. (2017). Suitable reference genes were selected, *glyceraldehyde 3-phosphate dehydrogenase (GAPDH), ubiquitin conjugating enzyme 10 (Ubi)* and *CG13320,* from a pool of candidate reference genes by means of the geNorm software (Van Hiel et al., 2009; Vandesompele et al., 2002). All qPCR results were calculated according to the comparative delta Ct method and a mix of all samples was used as a calibrator. qPCR was used to determine the tissue distribution of the *Schgr*-CRF-DHR transcript, in immature and mature adult locusts. GraphPad Prism 6 (GraphPad Software Inc.) was used to plot the data and to test the statistical significance, using ANOVA, of the observed differences between immature and mature transcript levels.

2.5. Molecular cloning of Schgr-CRF-DHR

The full-length sequence of *Schgr*-CRF-DHR was found in the *S. gregaria* transcriptome database, as described in 2.1. The complete ORF was PCR-amplified using cDNA of brains and Pwo DNA Polymerase (Roche). The nucleotide sequences of the specific forward primer, containing the CACC Kozak sequence at the 5' side to facilitate translation in mammalian cells (Kozak, 1986), and reverse primer, are enlisted in Supplementary Table S2. Amplicons were analyzed on a 1% agarose gel, purified using the GenElute Gel Extraction Kit (Sigma-Aldrich), cloned into a pcDNA3.1/V5-His-TOPO TA expression vector (Invitrogen) and transformed into One Shot TOP10 chemically competent *E. coli* cells (Invitrogen). The sequence of the insert was confirmed by Sanger sequencing. Bacteria harboring the correct receptor insert were grown overnight in LB medium supplemented with 100 ng/mL Ampicillin (Invitrogen), and plasmid DNA was isolated using the GenElute Plasmid Miniprep Kit (Sigma-Aldrich).

2.6. Cell culture and transfection

Pharmacological studies were carried out in a Chinese hamster ovary (CHO)-WTA11 cell line, genetically modified to stably express apo-aequorin, a zeocin resistance gene, and the promiscuous $G\alpha_{16}$ subunit coupling to the phospholipase C and Ca^{2+} signaling cascade (Euroscreen, Belgium). CHO-PAM28 cells (stably expressing apo-aequorin and a puromycin resistance gene) and human embryonic kidney (HEK) 293T cells were used to assess effects on the Ca^{2+} and/or cAMP second messenger systems, respectively.

Cell culture and transfections of CHO-WTA11 and CHO-PAM28 cells were performed as described by Lismont et al. (2015). HEK293T cells were cultured in monolayers at 37 °C with a constant supply of 5% CO_2 in 10 cm Nunc Cell Culture/Petri Dishes (Thermo Scientific) in DMEM (Gibco) supplemented with 1% fungizone (Gibco), 10% fetal bovine serum (FBS; Gibco), 1% sodium pyruvate (Invitrogen), and 1% penicillin/streptomycin (stock solution: 10 000 units/mL penicillin and 10 mg/mL streptomycin; Invitrogen). Cells were sub-cultured twice a week.

For the $BRET^1$-based CAMYEL biosensor assay, 5×10^6 HEK293T cells were transiently transfected using the calcium phosphate method (Jordan et al., 1996). Thus, cells were co-transfected with 4 μg CAMYEL vector, combined with 10 μg *Schgr*-CRF-DHR pcDNA3.1 receptor expression construct and 6 μg pcDNA3.1 TOPO empty vector or with 16 μg of pcDNA3.1 TOPO empty vector only. The cell medium was replaced with 10 mL fresh HEK293T culture medium half an hour prior to transfection and the DNA mixture was prepared in MilliQ water to a final volume of 500 μL.

For the $BRET^2$-based G protein biosensor analyses, HEK293T cells were co-transfected using the calcium phosphate method with (1) one of the ten Gα-Rluc8 constructs, $G\gamma_2$-GFP10, $G\beta_1$, pcDNA3.1: *Schgr*-CRF-DHR, constituting the experimental conditions, or (2) one of the ten Gα-Rluc8 constructs, $G\gamma_2$-GFP10, $G\beta_1$ and the pcDNA3.1 empty vector, constituting the control conditions. The ten Gα-Rluc8 constructs are: $G\alpha_{i1}$, $G\alpha_{i2}$, $G\alpha_{i3}$, $G\alpha_{oa}$, $G\alpha_{ob}$ representing the $G_{\alpha i/o}$ subfamily, $G_{\alpha 11}$ and $G_{\alpha q}$ representing the $G\alpha_{q/11}$ subfamily, $G\alpha_s$ as a representative of the G_s subfamily, and $G\alpha_{12}$ and $G\alpha_{13}$ representing the $G\alpha_{12/13}$ subfamily. In all cells, the G protein heterodimer $\alpha_x\ \beta_1\gamma_2$ is expressed with $G\alpha_x$ representing one of the ten Gα constructs. The cell medium was replaced half an hour prior to transfection with 10 mL fresh culture medium and the mixtures of DNA constructs were prepared as described in Supplementary table S3.1 for the experimental conditions, and in Supplementary table S3.2 for the controls. All mixtures were brought to a concentration of ~20 μg DNA in 500 μL MilliQ water.

For transfections using the calcium phosphate method, 50 μL $CaCl_2$ (2.5 M) was added to the DNA mixture. Next, 500 μL HEPES-buffered saline [HBS (2x); 280 mM NaCl, 50 mM HEPES and 1.5 mM Na_2HPO_4; pH 7.1] were added. The transfected cells were maintained in an incubator at 37 °C (5% CO2). An additional transfection was performed with 4 μg CAMYEL vector and 16 μg empty vector, without pcDNA3.1 receptor construct, as an extra control. The transfected cells were maintained in an incubator at 37 °C (5% CO2) and on the next day the medium was replaced by fresh culture medium.

2.7. Aequorin reporter assay in CHO cells

The aequorin reporter assay was performed as described by Lismont et al. (2015). This assay will be used to measure calcium mobilization after *Schgr*-CRF-DHR activation. Peptides (Table 1) were ordered from GL Biochem (Shanghai, China) at 95% purity and further purified by RP-HPLC fractions that were subsequently controlled by MALDI. The peptides (Table 1) were tested in a dilution series (0.01 fM −10 μM). Further analysis was performed using Graphpad Prism 6 (GraphPad Software Inc.).

2.8. $BRET^1$-based CAMYEL biosensor assay

The original BRET system described by Xu and co-workers (1999) is referred to as $BRET^1$ and uses *Renilla* luciferase (*R*luc) as a donor with benzyl-coelenterazine (coelenterazine *h*) as a substrate in combination with enhanced yellow fluorescent protein (EYFP). The $BRET^1$-based CAMYEL biosensor can be used to measure cAMP levels in living cells upon GPCR activation. The core of this biosensor consists of the cAMP-binding protein EPAC, flanked by the BRET probes *R*Luc and EYFP. The sensor changes conformation in response to increasing levels of cAMP, resulting in a decrease of BRET intensity. In this study, this biosensor is used to measure bioluminescent changes resulting from increasing intracellular cAMP levels upon exposure of cells, transfected with the *Schgr*-CRF-DHR expression vector (experimental condition), to increasing concentrations of *Schgr*-CRF-DH. As a negative control condition, cells were transfected with the CAMYEL biosensor only.

One day post-transfection, the co-transfected HEK293T cells were detached using PBS supplemented with 0.2% EDTA (pH 8.0) and collected in a falcon tube. The cells were pelleted for 4 min at 800 rpm and resuspended at a density of 0.5×10^6 cells/mL in DMEM/F-12 without phenolred (Gibco) supplemented with 1% fungizone (Gibco), 10% fetal bovine serum (FBS; Gibco), 1% sodium pyruvate (Invitrogen), and 1% penicillin/streptomycin. Cells were seeded in white MicroWell 96-Well Optical-Bottom Plates with Polymer Base (catalog no. 165306; Thermo Scientific) by adding 100 μL of the cell solution (~50 000 cells) to each well. Subsequently, the cells were incubated overnight at 37 °C (5% CO_2).

The actual experiment was conducted two days post-transfection. Experiments were performed in the presence of IBMX (end concentration 40 μM), to prevent cAMP breakdown, and coelenterazine *h* (end concentration 5 μM; Promega), which is used as a substrate for *R*luc.

The HEK293T cells were rinsed with PBS, and subsequently resuspended in PBS. Next, cells were incubated for 5 min with the IBMX/coelenterazine *h* mix prior to the addition of *Schgr*-CRF-DH peptide at different concentrations (0.10 nM - 1 μM). $BRET^1$ readings were collected 5 min after stimulation using the Mithras LB940 (Berthold Technologies) and the ratio of emission of YFP (520–570 nm) to *R*luc (370–480 nm) was calculated. The results are expressed as BRET fold-change, *i.e.* the ratio of the BRET signal evoked in response to addition of the neuropeptide, over the BRET signal induced in response to addition of the buffer only. Measurements were taken in duplicate per concentration of peptide in two independent transfections for both the experimental condition (with insect receptor), and the negative control (without insect receptor). Calculations were made using the output files from the Microwin2000 (Mikrotek) in Excel (Microsoft) and further analysis was performed using GraphPad Prism 6 (GraphPad Software Inc.).

2.9. $BRET^2$-based G protein biosensor assay

An advanced BRET system $(BRET)^2$ uses different GFP variants in combination with the coelenterazine variant DeepBlueC, also referred to as coelenterazine 400a, which permits the measurement of the acceptor emission spectrum without any overlap of the donor emission spectrum. The $BRET^2$-based G protein biosensors can be used to measure activation of G proteins in living cells by monitoring conformational changes of G proteins. This technology relies on the interdomain movement that occurs within heterotrimeric G proteins upon GDP/GTP exchange, resulting in a decrease of the BRET signal between probes inserted within Gα and Gγ subunits (Galés et al., 2006). This technology detects the early signaling event that occurs after receptor activation and permits discrimination between different G protein subtypes activated by a receptor. To test whether the $BRET^2$-based G protein biosensors react to insect GPCRs, enabling the detection of the activation of specific G proteins, a first screen was conducted whereby only one high dose of peptide (1 μM) was applied. This pilot experiment was

Table 1
Primary structure of the peptides used in the current study to activate of *Schgr*-CRF-DHR with respective EC_{50} values.

Neuropeptide Name	Amino acid sequence	EC50 value
***Schgr*-CRF-DH**	MGMGPSLSIVNPMDVLRQRLLLEIARRRLRDAEEQIKANKDFLQQIamide	30,65 nM
***Trica*-DH44-I**	AGALGESGASLSIVNSLDVLRNRLLLEIARKKAKEGANRNRQILLSLamide	0,42 mM
***Trica*-DH44-II**	SPTISITAPIDVLRKTWAKENMRKQMQINREYLKNLQamide	/
***Acypi*-DH44**	NGAMQGESPRSRPSLSIVNSLDVLRQKLMYEVARRHVDENQKVLSQNHQILKNLamide	8,8 mM

Abbreviations: *Schgr* = *Schistocerca gregaria*, *Trica* = *Tribolium castaneum* and *Acypi* = *Acyrthosiphon pisum*.

performed in two separate transfections [for both (1) the experimental condition with insect receptor and (2) the control without insect receptor] per Gα construct ($G\alpha_{i1}$, $G\alpha_{i2}$, $G\alpha_{i3}$, $G\alpha_{oa}$, $G\alpha_{ob}$, $G\alpha_{s}$, $G\alpha_{11}$, $G\alpha_{q}$, $G\alpha_{12}$ or $G\alpha_{13}$). When a significant reaction was obtained, a second screen was conducted in three separate transfections per Gα construct to examine whether the obtained reaction was dose-dependent by using several concentrations of peptide (0.10 nM–1 μM).

The experiment was conducted two days post-transfection. After removal of the culture medium, the HEK293T cells were detached using PBS supplemented with 0.2% EDTA (pH 8.0) and collected. The cells were pelleted by centrifugation (4 min, 1100 rpm) and resuspended to a concentration of 1 μg of proteins/mL. The concentration of proteins per sample was determined using the DC Protein Assay (BIO-RAD) according to the manufacturer's instructions.

In the first experiment, cells were distributed (80 μg of proteins per well) to four wells in a 96-well microplate (Black/White Isoplate-96 Black Frame White Well; PerkinElmer Life Sciences). To the first two wells, 10 μL PBS (Gibco) was added as a blank. To the remaining two wells, 1 μM *Schgr*-CRF-DH peptide dissolved in PBS was supplemented. Exactly 1 min later, 5 μM coelenterazine 400a/DeepBlueC (Gentaur) was added. $BRET^2$ between $Rluc_8$ (370–450 nm) and GFP_{10} (510–540 nm) was measured using an Infinite F200 reader (Tecan Group Ltd) 1 min after addition of the DeepBlueC. For each well, the $BRET^2$ signal was calculated as the ratio of emission of GFP_{10} to $Rluc_8$. The result of the blank was subtracted from the two other wells (resulting in a $\Delta BRET^2$ value). This experiment was performed in duplicate per transfection (two for each Gα construct) for both experimental and control cells.

A significant reduction in $\Delta BRET^2$ signal in the experimental cells (with insect receptor) compared to the control cells (without receptor) may indicate that there is an activation of the Gα protein. The $\Delta BRET^2$ signal of the control cells should remain at the zero level. The magnitude of the $BRET^2$ signal depends on the biosensor used. Therefore, the y-axis of the graphs is set in the same range as observed in earlier studies which use the same $BRET^2$-based G protein biosensors to test receptor signaling of the *Homo sapiens* chemokine receptor (*Homsa*-CCR2; Corbisier et al., 2015) for the $G\alpha_{i/o}$ subfamily, the *H. sapiens* β2-adrenergic receptor (*Homsa*-β2-AR; Saulière et al., 2012) for the $G\alpha_{s}$ subfamily, the *H. sapiens* angiotensin II type 1 receptor (*Homsa*-AT1R, Saulière et al., 2012) for the $G\alpha_{q/11}$ subfamily and the *H. sapiens* thromboxane TPα receptor (TPα-R; Saulière et al., 2012) for the $G\alpha_{12/13}$ subfamily.

If the $\Delta BRET^2$ signal is significantly reduced in comparison to the control, we can conclude that the biosensor is truly activated. Therefore, HEK293T cells were co-transfected again in triplicate with insect receptor and the G protein biosensor constructs. The protocol of this assay is similar to the procedure described above but instead of adding cells to four wells, cells were added to six wells to test multiple concentrations of peptide (0.10 nM - 1 μM) including the PBS that serves as a blank. The result of the blank (first well) was subtracted from the other wells to calculate $\Delta BRET^2$. This procedure was performed in duplicate per transfection (in three transfections for each Gα construct) and the data were analyzed using the Excel output file (Microsoft) and GraphPad Prism 6 (GraphPad Software Inc.).

2.10. G protein analysis in S. gregaria

All available *D. melanogaster* G protein subunit sequences were obtained from FlyBase (https://flybase.org/) and used as a query to scan a brain-specific transcriptome database of gregarious *S. gregaria* created by illumina-sequenced reads (unpublished data), to identify G protein subunit sequences in this species. All identified G protein subunit sequences are validated by using the online tool GprotPRED (http://aias.biol.uoa.gr/GprotPRED/) which is able to recognize Gα, Gβ and Gγ subunits and is able to assign Gα subunits to one of the four Gα protein subfamilies; namely $G\alpha_{i/o}$, $G\alpha_{s}$, $G\alpha_{q/11}$ or $G\alpha_{12/13}$ (Kostiou et al., 2016). In case that GprotPRED is unable to assign a Gα protein sequence to a Gα subfamily, the sequence is assigned to a Gα protein subfamily based on sequence identity with other insect Gα subunit sequences by using the BLAST tool on NCBI (https://blast.ncbi.nlm.nih.gov/Blast.cgi).

A multiple sequence alignment was constructed for $G\alpha_{i}$, $G\alpha_{o}$, $G\alpha_{s}$, $G\alpha_{q/11}$, $G\alpha_{12/13}$, Gβ and Gγ using sequences of the *H. sapiens* G protein subunits used to construct the $BRET^2$-based G protein biosensors, as well as all identified G protein subunit sequences of *S. gregaria*. Since there are three $G\alpha_{i}$ subtypes and two $G\alpha_{o}$ isoforms, sequences of the $G\alpha_{i}$ and $G\alpha_{o}$ are analyzed separately. Multiple sequence alignments and additional percent identity matrices are constructed as described in 2.1.

GenBank accession numbers of the *H. sapiens* G protein subunit sequences used to construct the $BRET^2$-based G protein biosensors which are studied in the multiple sequence alignment are *GenBank: P63096* for *Homsa*-$G\alpha_{i1}$, *GenBank: P04899* for *Homsa*-$G\alpha_{i2}$, *GenBank: P08754* for *Homsa*-$G\alpha_{i3}$, *GenBank: NP_066268.1* for *Homsa*-$G\alpha_{oa}$, *GenBank: NP_620073.2* for *Homsa*-$G\alpha_{ob}$, *GenBank: P63092* for *Homsa*-$G\alpha_{s}$, *GenBank: P50148* for *Homsa*-$G\alpha_{q}$, *GenBank: P29992* for *Homsa*-$G\alpha_{11}$, *GenBank: Q03113* for *Homsa*-$G\alpha_{12}$, *GenBank: Q14344* for *Homsa*-$G\alpha_{13}$, *GenBank: P62873*, for *Homsa*-$G\beta_{1}$, and *GenBank: P59768* for *Homsa*-$G\gamma_{1}$.

GenBank accession numbers of the *D. melanogaster* G protein subunit sequences used to identify *S. gregaria* G protein subunit sequences are *GenBank: CG10060* for *Drome*-$G\alpha_{i}$, *GenBank: CG2204* for *Drome*-$G\alpha_{o}$, *GenBank: CG2835* for *Drome*-$G\alpha_{s60A}$, *GenBank: CG12232* for *Drome*-$G\alpha_{73B}$, *GenBank: CG17759* for *Drome*-$G\alpha_{q}$, *GenBank: CG17760* for *Drome*- $G\alpha_{SD21019p}$, *GenBank: CG17678* for *Drome*-$G\alpha_{12/13}$, *GenBank: CG10545* for *Drome*-$G\beta_{1}$, *GenBank: CG8770* for *Drome*-$G\beta_{2}$, *GenBank: CG10763* for *Drome*-$G\beta_{5}$, *GenBank: CG8261* for *Drome*-$G\gamma_{1}$ and *GenBank: CG3694* for Drome-$G\gamma_{30A}$.

3. Results

3.1. Cloning and sequence analysis of Schgr-CRF-DHR

The complete open reading frame (ORF) of the *Schgr-CRF-DHR* was found in a *S. gregaria* transcriptome database (unpublished data) and was verified by Sanger sequencing (LGC genomics) of the PCR amplicons obtained using the primers listed in Supplementary Table S1. The ORF of the *Schgr-CRF-DHR* cDNA consists of 1293 nucleotides encoding a 430 amino acids-long receptor (Fig. 1). Transmembrane topology prediction revealed the presence of seven hydrophobic regions forming the α-helical transmembrane segments (TM1-7) characteristic of GPCRs (Krogh et al., 2001; Sonnhammer et al., 1998). BLASTx searches revealed similarities of the cloned *Schgr-CRF-DHR* with other insect CRF-

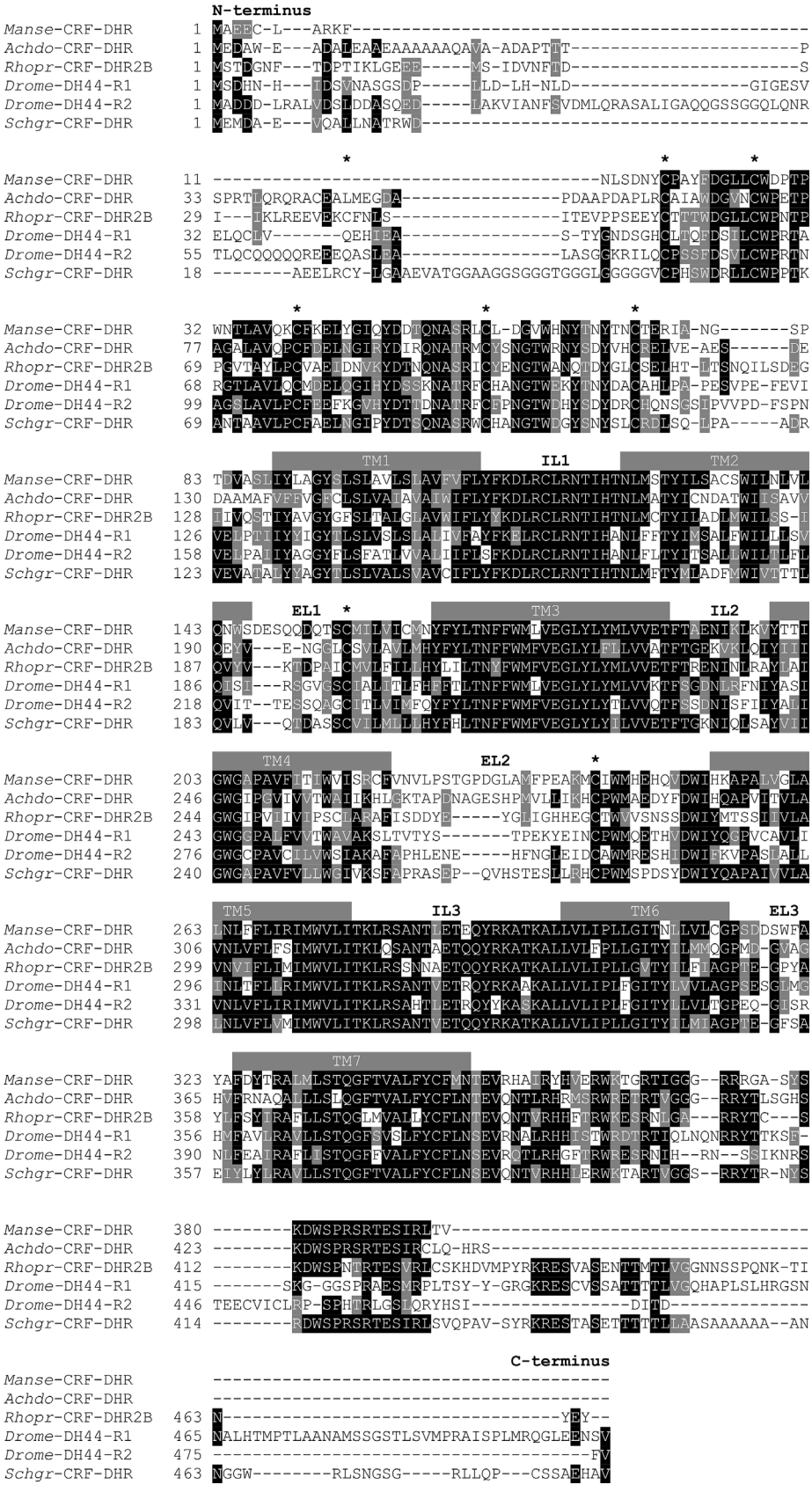

Fig. 2. Multiple sequence alignment of CRF-DHRs from *D. melanogaster* (Drome-DH44-R1; GenBank acc. no. NP_610960.1, and Drome-DH44-R2; GenBank acc. no. NP_610789.3), *R. prolixus* (Rhopr-CRF-DHR2B; GenBank acc. no. KJ407397), M. sexta (Manse-CRF-DHR; GenBank acc. no. AAC46469.1), *A. domesticus* (Achdo-CRF-DHR; GenBank acc. no AAC47000.1) and *S. gregaria* (*Schgr*-CRF-DHR). Identical residues between the aligned sequences are highlighted in black, and conservatively substituted residues in grey. Amino acid position is indicated at the left and dashes indicate gaps that are introduced to maximize similarities in the alignment. Putative transmembrane regions of *Schgr*-CRF-DHR and *Schgr*-CRF-DHR (TM1-TM7) are indicated by grey bars. Conserved cysteine residues that are predicted to form disulfide bridges in the N-terminus, EL1 and EL2 are indicated (*). The intracellular loops (IL) and the C-terminus of the receptors are shown as well.

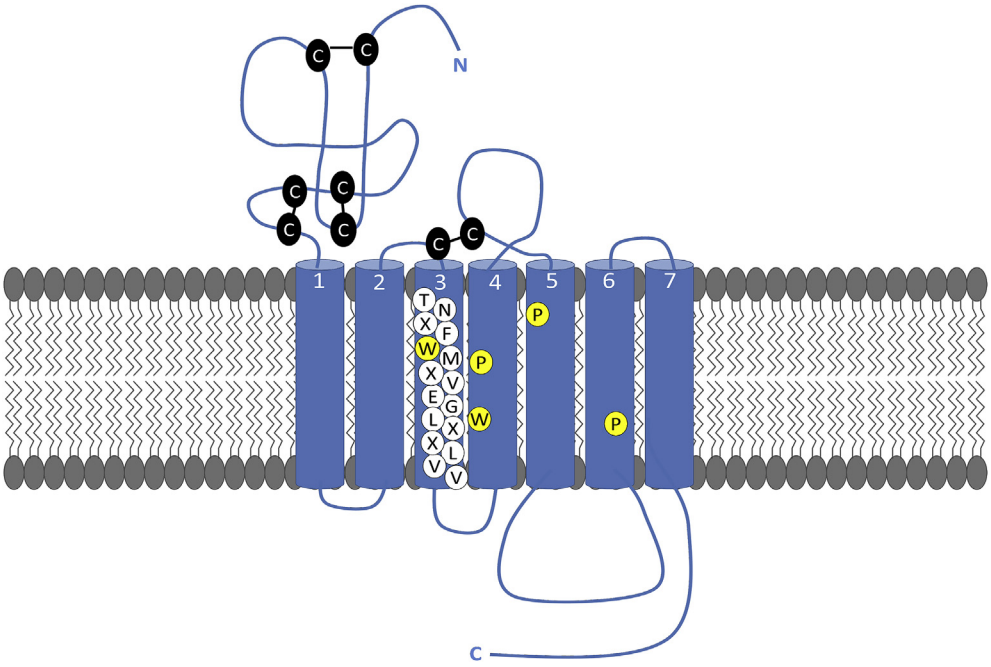

Fig. 3. Schematic representation of *Schgr*-CRF-DHR. *Schgr*-CRF-DHR is a secretin-like GPCR with seven transmembrane regions. The residues highlighted in yellow are a typical feature of secretin-like GPCRs. The highly conserved disulphide bridges in the N-terminus and a typical disulphide bridge formed between a cystein (C) at the beginning of transmembrane 3 and in extracellular loop 2, are indicated in black. The conserved TNXFWMXVELXXLVV motif in transmembrane 3 is accentuated in white, according to the multiple sequence alignment in Fig. 2. (For interpretation of the references to color in this figure legend, the reader is referred to the Web version of this article.)

DHRs. The *Schgr*-CRF-DHR sequence was submitted to GenBank at the National Center for Biotechnology Information (NCBI) and has received accession number *GenBank: MN663112*. A multiple sequence alignment with other *in vitro* functionally confirmed insect CRF-DH receptors is displayed in Fig. 2. *Schgr*-CRF-DHR displays the typical features of GPCRs belonging to the secretin receptor superfamily (Fig. 3). Insect CRF-DH receptors contain six conserved cysteine residues known to form disulfide bridges in the N-terminal region of all family B GPCRs, which is essential for ligand binding properties (Fredriksson et al., 2003). Furthermore, they contain two conserved cysteine residues in extracellular loop (EL)1 and EL2 known to form a disulfide bridge between these ELs, ensuring proper orientation of EL2 (Gether, 2000; Schiöth and Lagerström, 2008). The alignment (Fig. 2) shows that the *Schgr*-CRF-DHR sequence is highly conserved, especially in the transmembrane regions, the intracellular loops, and in some parts of the N- and C-terminal regions.

3.2. Transcript profiling

The tissue distribution of *Schgr*-CRF-DHR was studied in adult locusts using qRT-PCR. The results show that expression of *Schgr*-CRF-DHR is mainly restricted to the central nervous system (CNS) (Fig. 4). The relative transcript levels appear highest in the suboesophageal ganglion, the ventral nerve cord, the frontal ganglion and the brain, followed by a slightly lower expression in the optic lobes. The receptor transcript is also detected in the brain-associated endocrine organs, corpora cardiaca, corpora allata and prothoracic glands. However, no significant differences were found between the mature and immature female tissue samples that were compared in this study. No detectable relative expression levels were observed in the samples analyzed for peripheral tissues, such as fat body, flight muscle, intestine, epidermis, gonads and male accessory glands.

3.3. Pharmacological characterization of Schgr-CRF-DHR

3.3.1. The aequorin bioluminescence assay

Schgr-CRF-DHR elicits a sigmoidal dose-dependent response with an EC_{50} value in the high nanomolar range (30.65 nM, Table 1), when it is expressed in CHO-WTA11 cells (Fig. 5), indicating that *Schgr*-CRF-DH is an agonist of *Schgr*-CRF-DHR. However, no response is detected in CHO-PAM28 cells that do not contain the promiscuous $G\alpha_{16}$ protein (results not shown), which suggests that coupling of this receptor to a detectable elevation of intracellular Ca^{2+} levels may not occur via the signaling components that are endogenously present in this cell line.

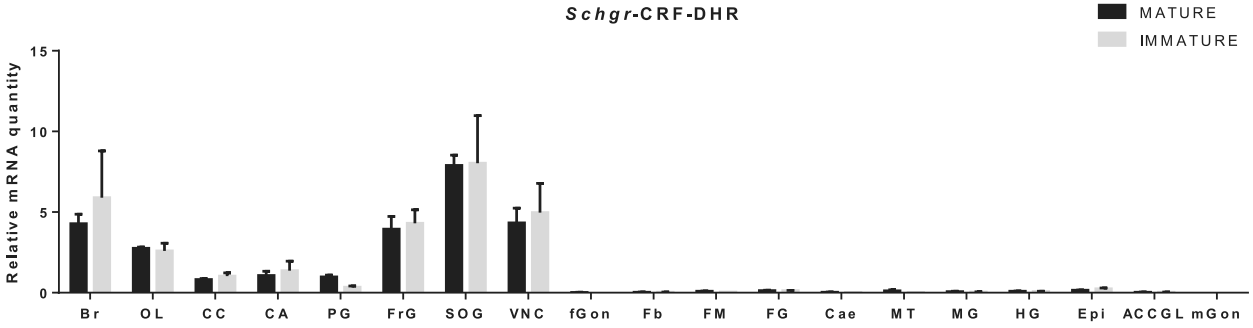

Fig. 4. Tissue distribution profile of *Schgr-CRF-DHR* in both immature and mature adult *S. gregaria*. The data represent mean values ± S.E.M. of three independent tissue samples run in duplicate, normalized relative to Ubi, CG13220 and GAPDH transcript levels. Significant differences between mature and immature samples were tested by ANOVA. Abbreviations used: Br = brain, OL = optic lobes, CC = corpora cardiaca, CA = corpora allata; PG = prothoracic glands, FrG = frontal ganglion, SOG = suboesophageal ganglion, VNC = ventral nerve cord, fGon = female gonads, FB = fat body, FM = flight muscle, FG = foregut, Cae = caecum, MT = Malpighian tubules, MG = midgut, HG = hindgut, Epi = epidermis, mGon = male gonads, ACCGL = male accessory glands.

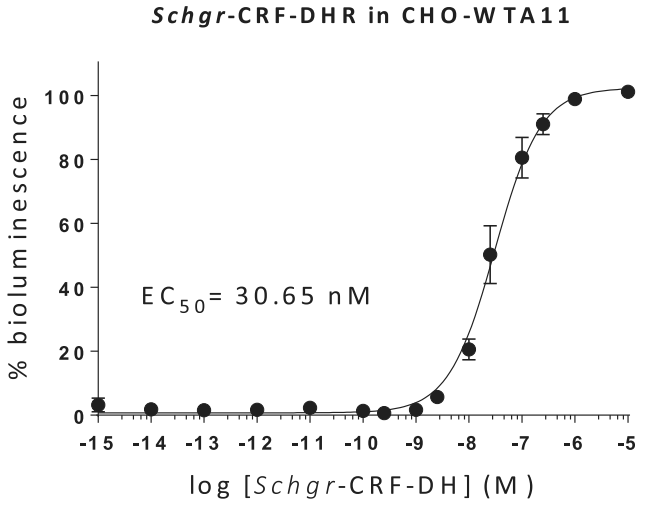

Fig. 5. Dose-response curve for aequorin-based bioluminescent responses induced in CHO-WTA11-*Schgr*-CRF-DHR cells. The aequorin bioluminescence assay is executed in two independent transfections. The bioluminescence is measured in triplicate per concentration of *Schgr*-CRF-DH and per transfection. Error bars represent the S.E.M and the 100% level refers to the maximal response level. The zero-response level corresponds to treatment with BSA medium only. In addition, the EC_{50} value is indicated.

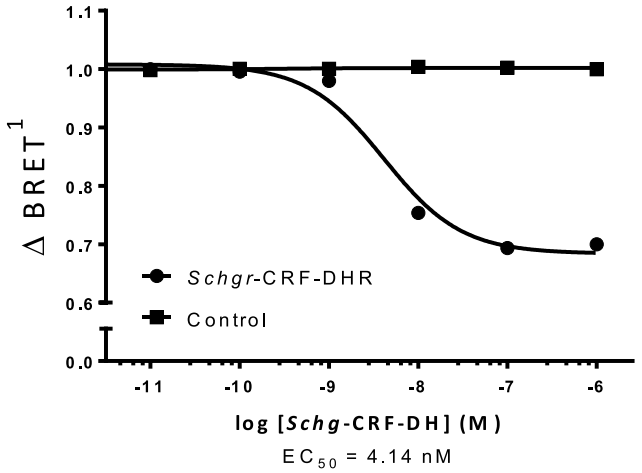

Fig. 6. Results of CAMYEL biosensor: BRET1 measured in HEK293T cells transfected with *Schgr*-CRF-DHR1 (●) or without *Schgr*-CRF-DHR1 [control (■)] in two independent transfections. Measurements are taken in duplicate for each concentration of *Schgr*-CRF-DH (10 pM - 1 μM). Data (± S.E.M) are presented relative to the baseline (buffer only).

In addition, CRF-DH-44 peptides derived from other insect species (Table 1), *Trica*-CRF-DH-I and *Trica*-CRF-DH-II from the red flour beetle *Tribolium castaneum*, and *Acypi*-CRF-DH from the pea aphid *Acyrthosiphon pisum*, were tested to investigate the ability of cross-species agonists to activate *Schgr*-CRF-DHR when it is expressed in CHO-WTA11 cells. We observed that *Trica*-CRF-DH-II (DH44-II) did not activate *Schgr*-CRF-DHR in the tested concentration range (Supplementary Fig. S1A). Furthermore, we observed partial sigmoidal activation of the locust receptor by *Trica*-CRF-DH-I and *Acypi*-CRF-DH (Supplementary Fig. S1A, with EC50 values in the (supra)micromolar range (0.42 μM and 8.8 μM, respectively; Table 1). There are some noticeable sequence differences between *Schgr*-CRF-DH and these other insect CRF-DH peptides (Supplementary Fig. S1B). For example, changes in the RLLL motif can be observed; in which Arg^{19} is replaced by Thr^{16} in *Trica*-DH44-II and by Lys^{27} in *Acypi*-DH44. Furthermore, Leu^{20} is replaced by Trp^{17} in *Trica*-DH44-II, and Leu^{22} is replaced by Lys^{19} in *Trica*-DH44-II and by Met^{29} in *Acypi*-DH44. In addition, changes in the charged amino acid RRLRD motif can be observed in *Acypi*-DH44 and *Trica*-DH44-I whereas this motif is deleted in *Trica*-DH44-II.

3.3.2. The CAMYEL biosensor

A dose-dependent decrease in $BRET^1$ signal is observed with an EC_{50} value in the nanomolar range (4.02 nM) in cells transfected with *Schgr*-CRF-DHR (Fig. 6). The control remains stable in the same range as the blank. These results suggest an increase in cAMP levels upon stimulation of *Schgr*-CRF-DHR by *Schgr*-CRF-DH.

3.3.3. Measuring a direct activation of the Gα protein by using $BRET^2$-based G protein biosensors

The $\Delta BRET^2$ signal measured in HEK293T-*Schgr*-CRF-DHR cells is reduced compared to the $\Delta BRET^2$ signal measured in the control cells upon addition of 1 μM *Schgr*-CRF-DH for four out of five biosensors ($G\alpha_{i2}$, $G\alpha_{i3}$, $G\alpha_{oa}$ and $G\alpha_{ob}$) of the $G\alpha_{i/o}$ subfamily (Fig. 7B-E). Moreover, the $\Delta BRET^2$ signals of $G\alpha_{i2}$, $G\alpha_{i3}$, $G\alpha_{oa}$ and $G\alpha_{ob}$ are dose-dependent with an EC_{50} value in the high nanomolar range (Fig. 8B–E), indicating that these biosensors are truly activated. Although the $\Delta BRET^2$ signal is decreased for the $G\alpha_{i1}$ biosensor (Fig. 7A) and a trend towards a reduced signal seems present when increasing concentrations of *Schgr*-CRF-DH are applied, no sigmoidal dose-dependent relationship is observed (Fig. 8A). In addition, a lower $\Delta BRET^2$ signal is measured for the $G\alpha_s$ biosensor in the HEK293T-*Schgr*-CRF-DHR cells when compared to the control cells (Fig. 7F). Moreover, this biosensor induces a dose-dependent decrease in $\Delta BRET^2$ signal with an EC_{50} value in the high nanomolar range (Fig. 8F), indicating that this biosensor is truly activated. Furthermore, neither the $G\alpha_{11}$ biosensor, nor the $G\alpha_q$ biosensor (Fig. 7G-H, Fig. 8G) appear to be activated.

When testing a single peptide dose, the $G\alpha_{12}$ biosensor generates a reduced $\Delta BRET^2$ signal in the HEK293T-*Schgr*-CRF-DHR cells compared to the control cells (Fig. 7I). However, when multiple concentrations of *Schgr*-CRF-DH are applied, no clear dose-dependence is detected (Fig. 8H). Finally, $G\alpha_{13}$ does not induce a significantly lower $\Delta BRET^2$ signal in the HEK293T-*Schgr*-CRF-DHR cells compared to the control cells (Fig. 7J).

3.3.4. Identification of G proteins in S. gregaria

To interpret the data of the $BRET^2$-based G protein biosensors, we also performed a BLAST analysis to identify G protein subunit sequences in the genome database of *D. melanogaster* and the transcriptome database of *S. gregaria* (unpublished data). The *Schgr*-Gα protein subunit sequences were submitted to GenBank at the National Center for Biotechnology Information (NCBI) and have received accession number *GenBank: MN663113* for *Schgr*-$G\alpha_i$, *GenBank: MN663114* for *Schgr*-$G\alpha_o$, *GenBank: MN663115* for *Schgr*-$G\alpha_s$, *GenBank: MN663116* for *Schgr*-$G\alpha_q$ and *GenBank: MN663117* for *Schgr*-$G\alpha_{12/13}$. By means of a multiple sequence alignment and a percent identity matrix, we compared these putative insect G protein subunit sequences with the human G protein subunit sequences that were used to construct the $BRET^2$-based G protein biosensors. We compared the G protein subunits per G protein subfamily, with the exception of the $G\alpha_{i/o}$ subfamily for which we analyzed the $G\alpha_i$ and $G\alpha_o$ sequences separately since this subfamily comprises five biosensors. Overall, the insect and human sequences of $G\alpha_i$, $G\alpha_o$, $G\alpha_s$ and $G\alpha_{q/11}$ subunits are very similar. The insect Gα protein subunits show a higher sequence identity with each other than with the human G protein subunits (Supplementary Figs. S2–S5 and Supplementary Tables S4–S7). They reported a sequence identity of 87% with the *D. melanogaster* $G\alpha_q$ subunit and a sequence identity of 80% with the human and mouse $G\alpha_q$ subunits.

However, insect and human members of the $G\alpha_{12/13}$ subfamily show less sequence identity than the other Gα protein subfamilies. Overall, the insect $G\alpha_{12/13}$ subunits only show a sequence identity of 51–59% with the human $G\alpha_{12}$ and $G\alpha_{13}$ subunits and of 62% with each

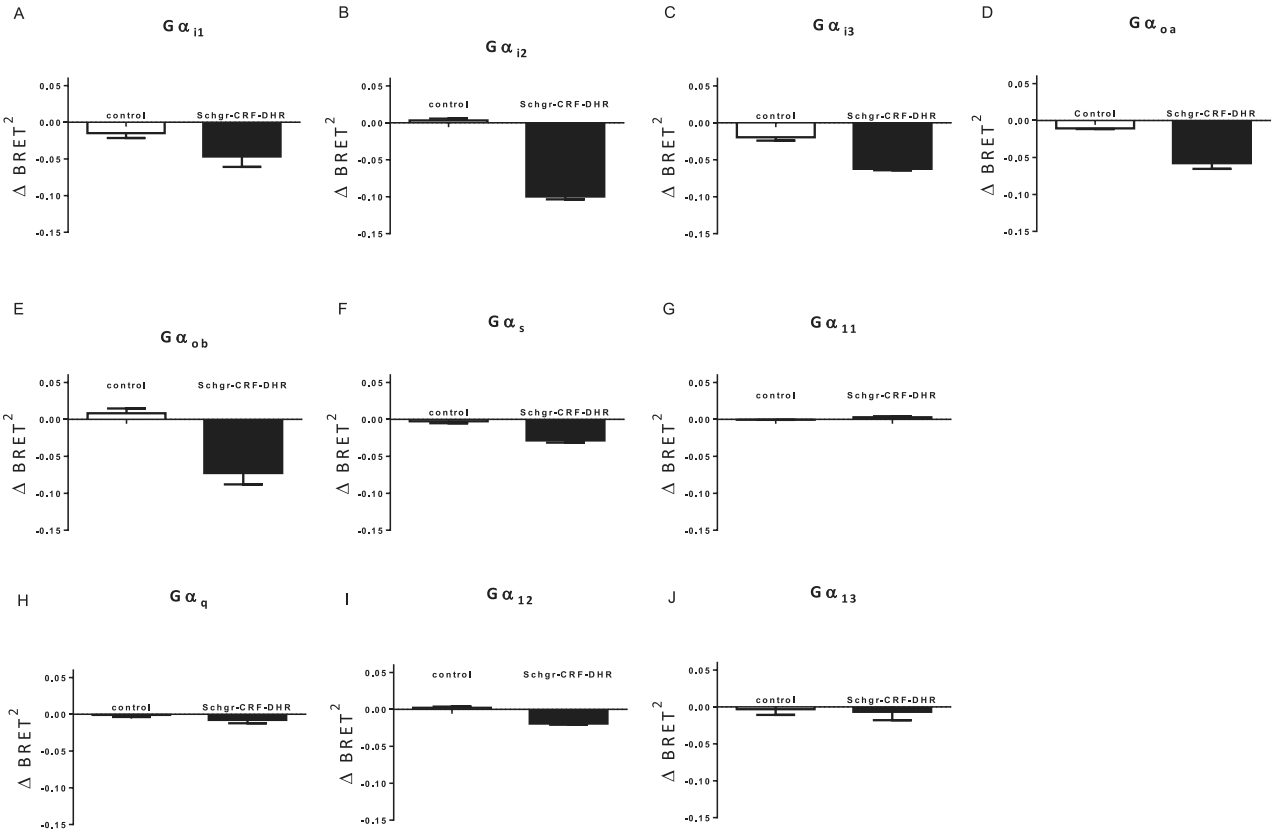

Fig. 7. Results of the HEK293T-*Schgr*-CRF-DHR cells (*Schgr*-CRF-DHR) and HEK293T cells (Control) co-transfected with BRET^2-based G protein biosensors upon stimulation of 1 μM *Schgr*-CRF-DH. A) $G\alpha_{i1}$ biosensor, B) $G\alpha_{i2}$ biosensor, C) $G\alpha_{i3}$ biosensor, D) $G\alpha_{oa}$ biosensor, E) $G\alpha_{ob}$ biosensor, F) $G\alpha_{s}$ biosensor, G) $G\alpha_{q}$ biosensor, H) $G\alpha_{11}$ biosensor, I) $G\alpha_{12}$ biosensor, J) $G\alpha_{13}$ biosensor. The data represent the means ± S.E.M of ΔBRET^2 measured in triplicate in two independent transfections.

other (Supplementary Fig. S6 and Supplementary Table S8).

In addition, we also identified two putative Gβ and two putative Gγ subunit sequences in the transcriptome database of *S. gregaria*. These *Schgr*-Gβ and *Schgr*-Gγ protein subunit sequences were submitted to GenBank at the National Center for Biotechnology Information (NCBI) and have received accession number *GenBank: MN663118* for *Schgr*-$G\beta_1$, *GenBank: MN663119* for *Schgr*-$G\beta_2$, *GenBank: MN663120* for *Schgr*-$G\gamma_1$ and *GenBank: MN663121* for *Schgr*-$G\gamma_2$. By looking at the multiple sequence alignment and the percent identity matrix, we concluded that *Schgr*-$G\beta_1$ and *Drome*-$G\beta_1$, with a sequence identity of 76–79% are more related to the *Homsa*-$G\beta_1$ subunit that was used to construct the BRET^2-based G protein biosensor. The same range of sequence identity is seen when different human Gβ subunit types are compared, *e.g.* when comparing four *Homsa*-$G\beta_{1\text{-}4}$ sequences 78–88% identity is observed. However, other insect β subunits, *Drome*-$G\beta_2$, *Drome*-$G\beta_5$ and *Schgr*-$G\beta_2$, only share a sequence identity of 40–55% of with this human subunit (Supplementary Fig. S7 and Supplementary Table S9).

We identified two putative Gγ sequences in *S. gregaria*, none of these is showing a high sequence identity with the human $G\gamma_2$ sequence that was used to construct the $G\gamma_2$-GFP10 biosensor (Supplementary Fig. S8 and Supplementary Table S10). The sequence identity of this human subunit merely ranges from 30% with *Drome*-γ_{30A} to 43% with *Drome*-$G\gamma_1$. Nevertheless, *Schgr*-$G\gamma_1$ and *Drome*-γ_1 on one hand and *Schgr*-$G\gamma_2$ and *Drome*-$G\gamma_{30A}$ on the other seem to be orthologues showing a sequence identity of 66% and 87.5%, respectively.

4. Discussion

4.1. Molecular cloning and receptor sequence analysis

In this study, *Schgr*-CRF-DHR was successfully cloned and characterized with cell-based functional receptor assays. As shown in the multiple sequence alignment (Fig. 2), the amino acid sequence of *Schgr*-CRF-DHR is well-conserved when compared with other insect CRF-DHRs that have been characterized *in vitro*: *Drome*-DH44-R1 and *Drome*-DH44-R2 (*D. melanogaster*), *Rhopr*-CRF-DHR2B (*R. prolixus*), *Manse*-CRF-DHR (*M. sexta*) and *Achdo*-CRF-DHR (*A. domesticus*), especially in the 7TM regions, parts of the N- and C-terminal regions, and the intracellular loops. The latter may be indicative for a conserved coupling of these receptors to downstream effectors, such as G proteins.

4.2. Tissue distribution analysis and functions of Schgr-CRF-DH

The distribution of the *Schgr*-CRF-DHR transcript (Fig. 4) is mainly restricted to the nervous system (Fig. 4). This is similar to *Drome-DH44-R1* distribution patterns that were mainly observed in the brain and VNC (Hector et al., 2009; Lee et al., 2015), and probably to *Aedae-DH44-R2* transcript abundance as well, which was solely detected in *A. aegypti* heads (Jagge and Pietrantonio, 2008). In addition, in line with the spatial expression profile of *Rhopr-CRF/DH-R2B* (Lee et al., 2016), gene expression of *Schgr-CRF-DHR* was also detected in different brain-associated endocrine organs. *Schgr-CRF-DHR* expression levels were also observed in the frontal ganglion, which belongs to the stomatogastric nervous system. However, no transcript levels were observed in Malpighian tubules or reproductive organs, which is in contrast to the spatial expression profile of *Rhopr-CRF/DH-R2B* (Lee et al., 2016).

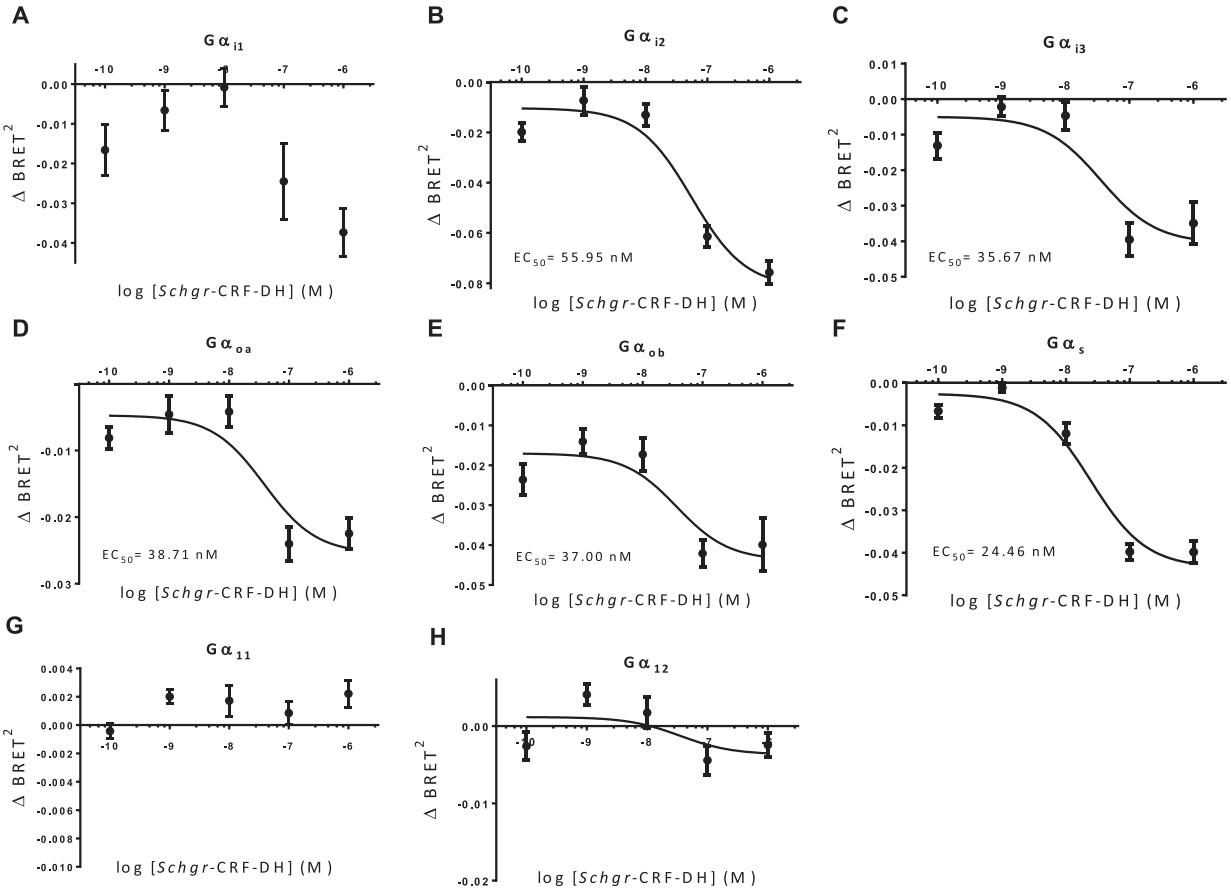

Fig. 8. Dose-dependent responses in HEK293T-*Schgr*-CRF-DHR1 cells co-transfected with BRET^2-based G protein biosensors consisting of $G\beta_1$, $G\gamma_2$-GFP10 and several Gα subunits upon stimulation of 0.01 nM–1 μM *Schgr*-CRF-DH. The data represent the means ± S.E.M of three independent transfections measured in duplicate per concentration. The EC50 value is indicated in case a dose-dependent reaction is observed.

Transcripts for *Drome-DH44-R2* (Hector et al., 2009) and *Aedae-DH44-R1* (Jagge and Pietrantonio, 2008) were also observed in Malpighian tubules.

Although CRF-DH plays a pronounced role in the regulation of diuresis, feeding, and reproduction in *S. gregaria* (Van Wielendaele et al., 2012) and other insects (Audsley et al., 1995, 1997; Te Brugge and Orchard, 2002; Goldsworthy et al., 2003; Tobe et al., 2005), this is not entirely reflected in the observed tissue distribution, since relative *Schgr*-CRF-DHR transcript levels are low or undetectable in several tissues that are involved in these processes. This infers that this is probably not the only *Schgr*-CRF-DH receptor, and/or that the peptide regulates some of these processes in an indirect manner. The former hypothesis is supported by the fact that in several insect species two distinct CRF-DH receptors have been identified (Caers et al., 2012; Hector et al., 2009; Jagge and Pietrantonio, 2008; Johnson et al., 2004; Lee et al., 2016), which can be an indication for a functional differentiation between both receptors. Moreover, differences in *in vitro* receptor signaling between both CRF-DHRs were observed in *D. melanogaster* (Hector et al., 2009) and *R. prolixus* (Lee et al., 2016). For instance, *Drome*-DH44-R2 is much more sensitive to *Drome*-DH44 than *Drome*-DH44-R1 and sensitivity of the latter to evoke a translocation of arrestin to the transmembrane is rather low. Furthermore, down-regulation of *Drome*-DH44-R2 by RNAi, results in a higher sensitivity to osmotic challenges in *D. melanogaster*. This agrees with the fact that expression of *Drome*-DH44-R2 is 200-fold higher in the Malpighian tubules than *Drome*-DH44-R1 (Hector et al., 2009). Alternatively, if *Schgr*-CRF-DHR would regulate physiological processes in an indirect manner, this could be obtained via neuronal control and/or via the regulation of the activity of endocrine organs.

High expression of *Schgr*-CRF-DHR in the brain, the optic lobes, the suboesophageal ganglion and the ventral nerve cord, suggests a prominent role for this receptor within the central nervous system. Moreover, expression levels are also high in the frontal ganglion, which is part of the stomatogastric nervous system. Both parts of the nervous system interact to regulate and coordinate the processes of feeding and digestion. The suboesophageal ganglion, for instance, innervates the mouthparts and the salivary glands and thus controls food intake (Audsley and Weaver, 2009; Nation, 2015). The frontal ganglion, on the other hand, innervates the foregut, enhancing gut motility and progression of the food bolus towards the midgut, where digestion and nutrient absorption are taking place (Holtof et al., 2019). Van Wielendaele et al. (2012) also point out that the decrease in food intake, as observed after injecting locusts with *Schgr*-CRF-DH, also may result from a decreased peripheral sensitivity to food stimuli, such as olfactory or gustatory stimuli, that affect central functions like appetite and feeding behavior.

4.3. Pharmacological receptor characterization and G protein mediated signaling pathways

The data obtained with the aequorin bioluminescence assay indicate that *Schgr*-CRF-DH is an agonist of *Schgr*-CRF-DHR and that activation of this receptor in absence of $G\alpha_{16}$ has no detectable effect on the PLC/Ca^{2+} pathway. This is in accordance with the available literature on other characterized CRF-DHRs in *R. prolixus* (Lee et al., 2016) and *D. melanogaster* (*i.e. Drome*-DH44-R2; Hector et al., 2009). In contrast, a stimulatory effect on the PLC/Ca^{2+} pathway has been reported for *Drome*-DH44-R1 (Hector et al., 2009).

In addition, we have analyzed the activity of three other CRF-DHs derived from the pest species, *T. casteneum* (*Trica*-CRF-DH-I and *Trica*-CRF-DH-II) and *A. pisum* (*Acypi*-CRF-DH). While CRF-DH peptides from these two insect species also display some agonistic activity to *Schgr*-CRF-DHR, our results point towards a much higher affinity of the desert locust CRF-DH peptide to *Schgr*-CRF-DHR, which is indicative for a long-term co-evolution between natural (locust) ligand-receptor couples (Markov et al., 2008). The observed higher cross-species activity between *Schgr*-CRF-DHR and *Trica*-CRF-DH-I (DH44-I) can probably be attributed to a higher structural similarity between this peptide and *Schgr*-CRF-DH in comparison to *Acypi*-CRF-DH (DH44) and *Trica*-CRF-DH-II (DH44-II). This is evidenced by amino acid sequence alignments, as well as by the sequence logos provided for CRF-DH in DINeR, a Database for Insect Neuropeptide Research (Yeoh et al., 2017). Clearly, when compared to *Schgr*-CRF-DH, the sequence of the least active (or even inactive) peptide, *Trica*-CRF-DH-II (DH44-II), is also the most divergent one (Supplementary Fig. S1B). The most noticeable difference in the sequence of this peptide is the substitution of various amino acids in the RLLL motif; Arg^{19}, a positively charged amino acid, is replaced by a polar uncharged Thr^{16} and the hydrophobic Leu^{23} residue is replaced by the positively charged Lys^{20} residue. In addition, hydrophobic Leu^{21} is replaced by a bigger hydrophobic amino acid Trp^{18}. Moreover, changes in the charged amino acid RRLRD motif can be observed in *Acypi*-DH44 and *Trica*-DH44-I. Most notably, the positively charged Arg^{30} residue is replaced by a negatively charged Asp residue in *Acypi*-DH44 and this motif is deleted in *Trica*-DH44-II. These amino acid substitutions might induce conformational changes within the analyzed peptides and/or might be intrinsic for binding capability to the *Schgr*-CRF-DHR. However, we cannot exclude that other structural motifs might also be of importance for ligand-receptor interaction, but this would require more detailed structural analyses.

The data obtained with the cAMP dependent CAMYEL biosensor assay indicate that cellular cAMP levels increase upon activation of *Schgr*-CRF-DHR by *Schgr*-CRF-DH. A stimulatory effect on cAMP levels is in agreement with the data previously reported for other *in vitro* characterized CRF-DHRs: activation of *Achdo*-CRF-DHR, *Manse*-CRF-DHR, *Rhopr*-CRF-DHR2B and both *Drome*-DH44-R1 and *Drome*-DH44-R2 by their respective peptide agonists induces the cAMP/protein kinase A pathway (Hector et al., 2009; Johnson et al., 2004; Lee et al., 2016; Reagan, 1995, 1996).

In addition, the downstream G protein mediated signaling pathways are studied in more detail using $BRET^2$-based G protein biosensors, which can measure direct activation of the G protein itself. The $G\alpha_s$ biosensor is activated in a dose-dependent manner upon exposure to *Schgr*-CRF-DH, in line with the results obtained for the CAMYEL biosensor-based assay. Interestingly, the magnitude of the $\Delta BRET^2$ signal is comparable with the magnitude of the $\Delta BRET^2$ signal detected with the *H. sapiens* β2-adrenergic receptor (Saulière et al., 2012), a receptor known to activate the $G\alpha_s$ protein. In addition, four out of five biosensors ($G\alpha_{i2}$, $G\alpha_{i3}$, $G\alpha_{oa}$ and $G\alpha_{ob}$) of the $G\alpha_{i/o}$ subfamily are activated in a dose-dependent manner when *Schgr*-CRF-DHR is stimulated by *Schgr*-CRF-DH. Notably, the magnitudes of the $\Delta BRET^2$ signals of the $G\alpha_{i/o}$ biosensors are also comparable to those previously detected with the *H. sapiens* chemokine receptors known to activate $G\alpha_{i/o}$ proteins (Corbisier et al., 2015). The fact that both $G\alpha_{i/o}$ and $G\alpha_s$ subfamilies are activated may appear contradictory. However, activation of the $G\alpha_{i/o}$ subfamily does not necessarily result in a decrease in intracellular cAMP levels. Together with the high conservation of metazoan $G\alpha_{i/o}$ subunits, the fact that this insect receptor can activate four mammalian members of this Gα subfamily suggests that it may also be capable of signaling to endogenous insect $G\alpha_{i/o}$ proteins. Clearly, this hypothesis remains to be confirmed for *in vivo* situations in the insect.

Furthermore, neither the $G\alpha_q$, nor the $G\alpha_{11}$ biosensor, both belonging to the $G\alpha_{q/11}$ subfamily, are activated by agonist-induced *Schgr*-CRF-DHR. This conclusion is further reinforced when the magnitude of the obtained $\Delta BRET^2$ signal (Fig. 7G and H) is compared to the magnitude of the $\Delta BRET^2$ signal detected with the *H. sapiens* angiotensin II type 1 receptor (Saulière et al., 2012), which is a receptor known to activate $G\alpha_{q/11}$ proteins. Moreover, this is in agreement with the results obtained with the aequorin bioluminescence assay in CHO-PAM28 cells.

In addition, no clear dose-dependent $\Delta BRET^2$ is observed with the $G\alpha_{12}$ biosensor when increasing concentrations of *Schgr*-CRF-DH are applied (Fig. 8H), particularly when the measured $\Delta BRET^2$ signal (Fig. 8H) is compared to the magnitude of the signal detected with the *H. sapiens* thromboxane TPα receptor (Saulière et al., 2012), which is a receptor known to activate $G\alpha_{12/13}$ proteins. Moreover, $G\alpha_{13}$, which belongs to the same subfamily, does not induce a significantly lower $BRET^2$ signal in the HEK293T-*Schgr*-CRF-DHR cells compared to the control cells. Whether this results from a lack of activation of members of the $G\alpha_{12/13}$ subfamily by this receptor type or from ineffective coupling of an insect receptor to mammalian $G\alpha_{12/13}$ subunits that display only limited structural conservation with their insect homologues, remains an open question.

These $BRET^2$-based G protein biosensors are also used to verify which specific Gα subunit isoform(s) can be activated within a particular Gα subunit family. However, only one $G\alpha_i$ and one $G\alpha_o$ subunit sequence are identified in *S. gregaria*. Therefore, knowledge of mammalian $G\alpha_i$ or $G\alpha_o$ isoform activation may not be very relevant for the natural situations encountered in insect cells and organisms. Overall, we conclude that the G protein subunit sequences of *D. melanogaster* and *S. gregaria* are more similar to each other than to their human counterparts. With exception of the $G\alpha_{12/13}$ subfamily, the Gα subunits show a high sequence similarity. The Gβ subunits seem to be less conserved, although it should be noted that *Homsa*-$G\beta_5$ also only shares a sequence identity of 51 – 53% with the four other *Homsa*-Gβ subunit isoforms (Dupré et al., 2009). The Gγ subunit sequences, on the other hand, display a very limited degree of conservation, especially between insects and humans. Nevertheless, since many insect receptors are being molecularly characterized in frequently cultured mammalian cell lines, this knowledge remains of high importance to allow for correct interpretations of *in vitro* receptor studies.

5. Conclusion

Taking all this together, we can conclude that a *Schgr*-CRF-DHR sequence was determined and validated *in vitro*. We have demonstrated that this locust neuropeptide receptor responds to its predicted agonist, *Schgr*-CRF-DH. Agonist-induced activation of the receptor has a stimulatory effect on the AC/cAMP pathway, but in absence of the promiscuous $G\alpha_{16}$ subunit it has no detectable effect on the PLC/Ca^{2+} pathway. These findings are in agreement with data obtained with the $BRET^1$-based CAMYEL biosensor (ATCC MBA-277), which appears to be very well suited for pharmacological characterization of this insect member of GPCR family B.

In addition, the cross-species agonist study might be indicative for the intrinsic potential of the *Schgr*-CRF-DHR to be selectively activated by an agonist. In the future, essential amino acids for receptor binding could be confirmed using peptide analogues (or similar techniques), as the identification of a target ligand binding site is an important step for structure-based rational agonist design for GPCRs. These essential characteristics might avoid or reduce non-target effects in case insecticides targeting this receptor would be developed in the future.

We have also shown that the $BRET^2$-based biosensor assays, consisting of the human $G\alpha_x$-$G\beta_1\gamma_2$ combinations, can accurately monitor the activation of an insect GPCR, the *Schgr*-CRF-DHR receptor. Nevertheless, although the different Gα subfamilies are highly conserved, with the exception of $G\alpha_{12/13}$, insect genomes tend to encode a lower number of isoforms within each subfamily. Moreover, Gβγ subunits appear to differ more profoundly from their mammalian counterparts, especially in comparison to the more conserved Gα subfamilies. Therefore, it might also prove to be useful to design $BRET^2$-

based biosensors with insect G proteins. By performing these assays in insect cells, the native structure and mode of action of both the GPCR and the G proteins would be respected.

Our study paves the way for further biosensor research, as well as for the future development of novel biosensors consisting of specific insect-derived components for studying insect GPCRs, thereby evoking the desired cellular responses in a signaling context that would more closely mimic the natural situation. Such assays might be of great value, for instance for analyzing the signaling characteristics and the application potential of novel insect pest-management compounds targeting this physiologically very important receptor category.

Acknowledgements

The authors are very grateful to Evelien Herinckx and all other Vanden Broeck team members for their assistance in the locust breeding. Special thanks go to Evert Bruyninckx, Paulien Peeters, Sander Maes, Pieter Van Wielendaele and Cynthia Lenaerts for excellent technical and practical assistance. The authors also gratefully acknowledge Marc Parmentier (University of Brussels, Belgium) and Michel Detheux (Euroscreen S.A., Belgium) for providing both CHO cell lines. Furthermore, the authors gratefully acknowledge Céline Galés (INSERM, Institut des Maladies Métaboliques et Cardiovasculaires, Université Paul Sabatier, Toulouse FRANCE) for providing all the BRET constructs.

Appendix A. Supplementary data

Supplementary data to this article can be found online at https://doi.org/10.1016/j.ibmb.2020.103392.

Funding

This work was financially supported by the Interuniversity Attraction Poles (IAP) programme (Belgian Science Policy Grant - P7/40), the European Union's Horizon 2020 Research and Innovation programme [No. 634361 (nEUROSTRESSPEP)], the Special Research Fund of KU Leuven (BOF grant) [C14/15/050], and the Research Foundation of Flanders (FWO), which also provided a postdoctoral research fellowship to HV and PhD fellowships to LV [VS.034.16N] and EV [1S64316N]. The Belgian 'Fonds pour la formation à la Recherche dans l'Industrie et l'Agriculture' (FRIA) provided PhD fellowships to JC and G-N D.

References

Audet, N., Galés, C., Archer-Lahlou, E., Vallières, M., Schiller, P.W., Bouvier, M., Pineyro, G., 2008. Bioluminescence resonance energy transfer assays reveal ligand-specific conformational changes within preformed signaling complexes containing delta-opioid receptors and heterotrimeric G proteins. J. Biol. Chem. 283, 15078–15088. https://doi.org/10.1074/jbc.M707941200.

Audsley, N., Weaver, R.J., 2009. Neuropeptides associated with the regulation of feeding in insects. Gen. Comp. Endocrinol. 162, 93–104. https://doi.org/10.1016/j.ygcen.2008.08.003.

Audsley, N., Kay, I., Hayes, T.K., Coast, G.M., 1995. Cross reactivity studies of CRF-related peptides on insect Malpighian tubules. Comp. Biochem. Physiol. Part A Physiol. 110, 87–93. https://doi.org/10.1016/0300-9629(94)00132-D.

Audsley, N., Goldsworthy, G.J., Coast, G.M., 1997. Circulating levels of *Locusta* diuretic hormone: the effect of feeding. Peptides 18, 59–65. https://doi.org/10.1016/S0196-9781(96)00234-3.

Baldwin, D.C., Schegg, K.M., Furuya, K., Lehmberg, E., Schooley, D.A., 2001. Isolation and identification of a diuretic hormone from *Zootermopsis nevadensis*. Peptides 22, 147–152. https://doi.org/10.1016/S0196-9781(00)00371-5.

Bellot, M., Galandrin, S., Boularan, C., Matthies, H.J., Despas, F., Denis, C., Javitch, J., Mazères, S., Sanni, S.J., Pons, V., Seguelas, M.-H., Hansen, J.L., Pathak, A., Galli, A., Sénard, J.-M., Galés, C., 2015. Dual agonist occupancy of AT1-R–α2C-AR heterodimers results in atypical Gs-PKA signaling. Nat. Chem. Biol. 11, 271–279. https://doi.org/10.1038/nchembio.1766.

Beyenbach, K.W., 1995. Mechanism and regulation of electrolyte transport in Malpighian tubules. J. Insect Physiol. 41, 197–207. https://doi.org/10.1016/0022-1910(94)00087-W.

Bil, M., Timmermans, I., Verlinden, H., Huybrechts, R., 2016. Characterization of the adipokinetic hormone receptor of the anautogenous flesh fly , *Sarcophaga crassipalpis*. J. Insect Physiol. 89, 52–59. https://doi.org/10.1016/j.jinsphys.2016.04.001.

Bruzzone, A., Saulière, A., Finana, F., Sénard, J.-M., Lüthy, I., Galés, C., 2014. Dosage-dependent regulation of cell proliferation and adhesion through dual β_2 -adrenergic receptor/cAMP signals. Faseb. J. 28, 1342–1354. https://doi.org/10.1096/fj.13-239285.

Busnelli, M., Saulière, A., Manning, M., Bouvier, M., Galés, C., Chini, B., 2012. Functional selective oxytocin-derived agonists discriminate between individual G protein family subtypes. J. Biol. Chem. 287, 3617–3629. https://doi.org/10.1074/jbc.M111.277178.

Caers, J., Verlinden, H., Zels, S., Vandersmissen, H.P., Vuerinckx, K., Schoofs, L., 2012. More than two decades of research on insect neuropeptide GPCRs : an overview. Front. Endocrinol. 3, 151. https://doi.org/10.3389/fendo.2012.00151.

Caers, J., Janssen, T., Van Rompay, L., Broeckx, V., Van Den Abbeele, J., Gäde, G., Schoofs, L., Beets, I., 2016a. Characterization and pharmacological analysis of two adipokinetic hormone receptor variants of the tsetse fly, *Glossina morsitans morsitans*. Insect Biochem. Mol. Biol. 70, 73–84. https://doi.org/10.1016/j.ibmb.2015.11.010.

Caers, J., Van Hiel, M.B., Peymen, K., Zels, S., Van Rompay, L., Van Den Abbeele, J., Schoofs, L., Beets, I., 2016b. Characterization of a neuropeptide F receptor in the tsetse fly, *Glossina morsitans morsitans*. J. Insect Physiol. 93–94, 105–111. https://doi.org/10.1016/j.jinsphys.2016.09.013.

Cannell, E., Dornan, A.J., Halberg, K.A., Terhzaz, S., Dow, J.A.T., Davies, S., 2016. The Corticotropin-releasing factor-like diuretic hormone 44 (DH44) and kinin neuropeptides modulate desiccation and starvation tolerance in *Drosophila melanogaster*. Peptides 80, 96–107. https://doi.org/10.1016/j.peptides.2016.02.004.

Capra, V., Busnelli, M., Perenna, A., Ambrosio, M., Accomazzo, M.R., Chini, B., Rovati, G.E., 2013. Full and partial agonists of thromboxane prostanoid receptor unveil fine Tuning of receptor Superactive conformation and G protein activation. PloS One 8, e60475. https://doi.org/10.1371/journal.pone.0060475.

Clottens, F.L., Holman, G.M., Coast, G.M., Totty, N.F., Hayes, T.K., Kay, I., Mallet, A.I., Wright, M.S., Chung, J.S., Truong, O., Bull, D.L., 1994. Isolation and characterization of a diuretic peptide common to the house fly and stable fly. Peptides 15, 971–979. https://doi.org/10.1016/0196-9781(94)90059-0.

Coast, G.M., Kay, I., 1994. The effects of *Acheta* diuretic peptide on isolated malpighian tubules from the house cricket *Acheta domesticus*. J. Exp. Biol. 187, 225–243.

Corbisier, J., Huszagh, A., Parmentier, M., Springael, J., 2015. Biased signaling at chemokine receptors. J. Biol. Chem. 290, 9542–9554. https://doi.org/10.1074/jbc.M114.596098.

Cullen, D.A., Cease, A.J., Latchininsky, A.V., Ayali, A., Berry, K., Buhl, J., De Keyser, R., Foquet, B., Hadrich, J.C., Matheson, T., Ott, S.R., Poot-Pech, M.A., Robinson, B.E., Smith, J.M., Song, H., Sword, G.A., Vanden Broeck, J., Verdonck, R., Verlinden, H., Rogers, S.M., 2017. From molecules to management: mechanisms and consequences of locust phase polyphenism. Adv. Insect Physiol 53, 167–285. https://doi.org/10.1016/bs.aiip.2017.06.002.

Damian, M., Mary, S., Maingot, M., M'Kadmi, C., Gagne, D., Leyris, J.-P., Denoyelle, S., Gaibelet, G., Gavara, L., Garcia de Souza Costa, M., Perahia, D., Trinquet, E., Mouillac, B., Galandrin, S., Galès, C., Fehrentz, J.-A., Floquet, N., Martinez, J., Marie, J., Banères, J.-L., 2015. Ghrelin receptor conformational dynamics regulate the transition from a preassembled to an active receptor:G_q complex. Proc. Natl. Acad. Sci. Unit. States Am. 112, 1601–1606. https://doi.org/10.1073/pnas.1414618112.

De Henau, O., Degroot, G.-N., Imbault, V., Robert, V., De Poorter, C., Mcheik, S., Galés, C., Parmentier, M., Springael, J.-Y., 2016. Signaling properties of Chemerin receptors CMKLR1, GPR1 and CCRL2. PloS One 11, e0164179. https://doi.org/10.1371/journal.pone.0164179.

Denis, C., Sauliere, A., Galandrin, S., Senard, J.-M., Gales, C., 2012. Probing heterotrimeric G-protein activation: Applications to biased ligands. Curr. Pharmaceut. Des. 18, 128–144. https://doi.org/10.2174/138161212799040466.

Dillen, S., Zels, S., Verlinden, H., Spit, J., Van Wielendaele, P., Vanden Broeck, J., 2013. Functional characterization of the short neuropeptide F receptor in the desert locust , Schistocerca gregaria. PLoS One 8, e53604. https://doi.org/10.1371/journal.pone.0053604.

Dupré, D.J., Robitaille, M., Rebois, R.V., Hébert, T.E., 2009. The role of Gβγ subunits in the organization, assembly, and function of GPCR signaling complexes. Annu. Rev. Pharmacol. Toxicol. 49, 31–56. https://doi.org/10.1146/annurev-pharmtox-061008-103038.

Fredriksson, R., Lagerström, M.C., Lundin, L.G., Schiöth, H.B., 2003. The G-protein-coupled receptors in the human genome form five Main Families . Phylogenetic analysis , paralogon Groups , and Fingerprints. Mol. Pharmacol. 63, 1256–1272.

Furuya, K., Milchak, R.J., Schegg, K.M., Zhang, J., Tobe, S.S., Coast, G.M., Schooley, D.A., 2000. Cockroach diuretic hormones : characterization of a calcitonin-like peptide in insects. Proc. Natl. Acad. Sci. Unit. States Am. 97, 6469–6474. https://doi.org/10.1073/pnas.97.12.6469.

Gäde, G., Goldsworthy, G.J., 2003. Insect peptide hormones : a selective review of their physiology and potential application for pest control. Pest Manag. Sci. 59, 1063–1075. https://doi.org/10.1002/ps.755.

Galandrin, S., Oligny-Longpré, G., Bonin, H., Ogawa, K., Galés, C., Bouvier, M., 2008. Conformational rearrangements and signaling cascades involved in ligand-biased mitogen-activated protein kinase signaling through the beta1-adrenergic receptor. Mol. Pharmacol. 74, 162–172. https://doi.org/10.1124/mol.107.043893.

Galandrin, S., Denis, C., Boularan, C., Marie, J., M'Kadmi, C., Pilette, C., Dubroca, C., Nicaise, Y., Seguelas, M.H., N'Guyen, D., Banères, J.L., Pathak, A., Sénard, J.M., Galés, C., 2016. Cardioprotective angiotensin-(1-7) peptide acts as a natural-biased ligand at the angiotensin II type 1 receptor. Hypertension 68, 1365–1374. https://doi.org/10.1161/HYPERTENSIONAHA.116.08118.

Galés, C., Van Durm, J.J.J., Schaak, S., Pontier, S., Percherancier, Y., Audet, M., Paris, H.,

Bouvier, M., 2006. Probing the activation-promoted structural rearrangements in preassembled receptor–G protein complexes. Nat. Struct. Mol. Biol. 13, 778–786. https://doi.org/10.1038/nsmb1134.
Garcia, C., Maurel-Ribes, A., Nauze, M., N'Guyen, D., Martinez, L.O., Payrastre, B., Sénard, J.-M., Galés, C., Pons, V., 2018. Deciphering biased inverse agonism of cangrelor and ticagrelor at $P2Y_{12}$ receptor. Cell. Mol. Life Sci. 76, 561–576. https://doi.org/10.1007/s00018-018-2960-3.
Gether, U., 2000. Uncovering molecular mechanisms involved in activation of G protein-coupled receptors. Endocr. Rev. 21, 90–113. https://doi.org/10.1210/er.21.1.90.
Goldsworthy, G.J., Chung, J.S., Simmonds, M.S.J., Tatari, M., Varouni, S., Poulos, C.P., 2003. The synthesis of an analogue of the locust CRF-like diuretic peptide, and the biological activities of this and some C-terminal fragments. Peptides 24, 1607–1613. https://doi.org/10.1016/j.peptides.2003.09.010.
Hansen, J.T., Lyngsø, C., Speerschneider, T., Hansen, P.B.L., Weiner, D.M., Sheikh, S.P., Burstein, E.S., Hansen, J.L., 2013. Functional Enhancement of AT1R potency in the presence of the TP a R is revealed by a Comprehensive 7TM receptor Co-expression screen. PloS One 8, 1–11. https://doi.org/10.1371/journal.pone.0058890.
Hector, C.E., Bretz, C.A., Zhao, Y., Johnson, E.C., 2009. Functional differences between two CRF-related diuretic hormone receptors in *Drosophila*. J. Exp. Biol. 212, 3142–3147. https://doi.org/10.1242/jeb.033175.
Holtof, M., Lenaerts, C., Cullen, D., Vanden Broeck, J., 2019. Extracellular nutrient digestion and absorption in the insect gut. Cell Tissue Res. 377, 397–414. https://doi.org/10.1007/s00441-019-03031-9.
Horodyski, F.M., Verlinden, H., Filkin, N., Vandersmissen, H.P., Fleury, C., Reynolds, S.E., Kai, Z., Vanden Broeck, J., 2011. Isolation and functional characterization of an allatotropin receptor from *Manduca sexta*. Insect Biochem. Mol. Biol. 41, 804–814. https://doi.org/10.1016/j.ibmb.2011.06.002.
Huang, J., Marchal, E., Hult, E.F., Zels, S., Vanden Broeck, J., Tobe, S.S., 2014. Mode of action of allatostatins in the regulation of juvenile hormone biosynthesis in the cockroach, *Diploptera punctata*. Insect Biochem. Mol. Biol. 54, 61–68. https://doi.org/10.1016/j.ibmb.2014.09.001.
Jagge, C.L., Pietrantonio, P.V., 2008. Diuretic hormone 44 receptor in Malpighian tubules of the mosquito Aedes aegypti : evidence for transcriptional regulation paralleling urination. Insect Mol. Biol. 17, 413–426. https://doi.org/10.1111/j.1365-2583.2008.00817.x.
Jiang, L.I., Collins, J., Davis, R., Lin, K.M., DeCamp, D., Roach, T., Hsueh, R., Rebres, R.A., Ross, E.M., Taussig, R., Fraser, I., Sternweis, P.C., 2007. Use of a cAMP BRET sensor to characterize a novel regulation of cAMP by the sphingosine 1-phosphate/G13 pathway. J. Biol. Chem. 282, 10576–10584. https://doi.org/10.1074/jbc.M609695200.
Johannessen, M., Delghandi, M.P., Moens, U., 2004. What turns CREB on? Cell. Signal. 16, 1211–1227. https://doi.org/10.1016/j.cellsig.2004.05.001.
Johnson, E.C., Bohn, L.M., Taghert, P.H., 2004. *Drosophila* CG8422 encodes a functional diuretic hormone receptor. J. Exp. Biol. 207, 743–748. https://doi.org/10.1242/jeb.00818.
Jordan, M., Schallhorn, A., Wurm, F.M., Francisco, S.S., 1996. Transfecting mammalian cells : optimization of critical parameters affecting calcium-phosphate precipitate formation. Nucleic Acids Res. 24, 596–601. https://doi.org/10.1093/nar/24.4.569.
Kim, Y., Galizia, C.G., Cho, K., Adams, M.E., 2006. Article A Command chemical Triggers an innate behavior by Sequential activation of multiple peptidergic Ensembles. Curr. Biol. 16, 1395–1407. https://doi.org/10.1016/j.cub.2006.06.027.
Kostiou, V.D., Theodoropoulou, M.C., Hamodrakas, S.J., 2016. GprotPRED: Annotation of Gα, Gβ and Gγ subunits of G-proteins using profile Hidden Markov Models (pHMMs) and application to proteomes. Biochim. Biophys. Acta Protein Proteonomics 1864, 435–440. https://doi.org/10.1016/J.BBAPAP.2016.02.005.
Kozak, M., 1986. Point mutations define a sequence flanking the AUG initiator codon that modulates translation by eukaryotic ribosomes. Cell 44, 283–292. https://doi.org/10.1016/0092-8674(86)90762-2.
Krogh, A., Larsson, È., von Heijne, G., Sonnhammer, E.L.L., 2001. Predicting transmembrane protein topology with a hidden Markov Model : application to complete genomes. J. Mol. Biol. 19, 567–580. https://doi.org/10.1006/jmbi.2000.4315.
Leduc, M., Breton, B., Gouill, C. Le, Bouvier, M., Chemtob, S., Heveker, N., 2009. Functional Selectivity of natural and Synthetic prostaglandin EP 4 receptor ligands. J. Pharmacol. Exp. Therapeut. 331, 297–307. https://doi.org/10.1124/jpet.109.156398.
Lee, K., Daubnerova, I., Chung, J., Kim, Y., Isaac, R.E., 2015. A neuronal pathway that controls sperm Ejection and storage in female *Drosophila* A neuronal pathway that controls sperm Ejection and storage in female *Drosophila*. Curr. Biol. 25, 790–797. https://doi.org/10.1016/j.cub.2015.01.050.
Lee, H., Zandawala, M., Lange, A.B., Orchard, I., 2016. Isolation and characterization of the corticotropin-releasing factor-related diuretic hormone receptor in *Rhodnius prolixus*. Cell. Signal. 28, 1152–1162. https://doi.org/10.1016/j.cellsig.2016.05.020.
Lenaerts, C., Cools, D., Verdonck, R., Verbakel, L., Vanden Broeck, J., Marchal, E., 2017. The ecdysis triggering hormone system is essential for successful moulting of a major hemimetabolous pest insect, *Schistocerca gregaria*. Sci. Rep. 7, 46502. https://doi.org/10.1038/srep46502.
Lismont, E., Vleugels, R., Marchal, E., Badisco, L., Van Wielendaele, P., Lenaerts, C., Zels, S., Tobe, S.S., Vanden Broeck, J., Verlinden, H., 2015. Molecular cloning and characterization of the allatotropin precursor and receptor in the desert locust, *Schistocerca gregaria*. Front. Neurosci. 9, 84. https://doi.org/10.3389/fnins.2015.00084.
Lismont, E., Mortelmans, N., Verlinden, H., Vanden Broeck, J., 2018. Molecular cloning and characterization of the SIFamide precursor and receptor in a hymenopteran insect, Bombus terrestris. Gen. Comp. Endocrinol. 258, 39–52. https://doi.org/10.1016/j.ygcen.2017.10.014.
Marchal, E., Schellens, S., Monjon, E., Bruyninckx, E., Marco, H.G., Gäde, G., Vanden Broeck, J., Verlinden, H., 2018. Analysis of peptide ligand specificity of different insect adipokinetic hormone receptors. Int. J. Mol. Sci. 19, e542. https://doi.org/10.3390/ijms19020542.
Markov, G.V., Paris, M., Bertrand, S., Laudet, V., 2008. The evolution of the ligand/receptor couple : a long road from comparative endocrinology to comparative genomics. Mol. Cell. Endocrinol. 293, 5–16. https://doi.org/10.1016/j.mce.2008.06.011.
Matthiesen, K., Nielsen, J., 2011. Cyclic AMP control measured in two compartments in HEK293 cells: phosphodiesterase K_M is more important than phosphodiesterase localization. PloS One 6, e24392. https://doi.org/10.1371/journal.pone.0024392.
Maurice, P., Daulat, A.M., Turecek, R., Ivankova-Susankova, K., Zamponi, F., Kamal, M., Clement, N., Guillaume, J.-L., Bettler, B., Galès, C., Delagrange, P., Jockers, R., 2010. Molecular organization and dynamics of the melatonin MT_1 receptor/RGS20/G_i protein complex reveal asymmetry of receptor dimers for RGS and G_i coupling. EMBO J. 29, 3646–3659. https://doi.org/10.1038/emboj.2010.236.
Meeusen, T., Mertens, I., Clynen, E., Baggerman, G., Nichols, R., Nachman, R.J., Huybrechts, R., De Loof, A., Schoofs, L., 2002. Identification in *Drosophila melanogaster* of the invertebrate G protein-coupled FMRFamide receptor. Proc. Natl. Acad. Sci. Unit. States Am. 99, 15363–15638. https://doi.org/10.1073/pnas.252339599.
Mertens, I., Meeusen, T., Huybrechts, R., De Loof, A., Schoofs, L., 2002. Characterization of the short neuropeptide F receptor from *Drosophila melanogaster*. Biochem. Biophys. Res. Commun. 297, 1140–1148. https://doi.org/10.1016/S0006-291X(02)02351-3.
Mollayeva, S., Orchard, I., Lange, A.B., 2018. The involvement of *Rhod*-CRF/DH in feeding and reproduction in the blood-gorging insect *Rhodnius prolixus*. Gen. Comp. Endocrinol. 258, 79–90. https://doi.org/10.1016/j.ygcen.2017.07.005.
Nation, J.L., 2015. Insect Physiology and Biochemistry, third. ed. CRC Press, Boca Raton.
Onfroy, L., Galandrin, S., Pontier, S.M., Seguelas, M.-H., N'Guyen, D., Sénard, J.-M., Galés, C., 2017. G protein stoichiometry dictates biased agonism through distinct receptor-G protein partitioning. Sci. Rep. 7, 7885. https://doi.org/10.1038/s41598-017-07392-5.
O'Donnell, M.J., Dow, J.A., Huesmann, G.R., Tublitz, N.J., Maddrell, S.H., 1996. Separate control of anion and cation transport in Malpighian tubules of *Drosophila melanogaster*. J. Exp. Biol. 199, 1163–1175.
Peverelli, E., Busnelli, M., Vitali, E., Giardino, E., Galés, C., Lania, A.G., Beck-Peccoz, P., Chini, B., Mantovani, G., Spada, A., 2013. Specific roles of G_i protein family members revealed by dissecting SST5 coupling in human pituitary cells. J. Cell Sci. 126, 638–644. https://doi.org/10.1242/jcs.116434.
Pierce, K.L., Premont, R.T., Lefkowitz, R.J., Hughes, T.H., 2002. Seven-transmembrane receptors. Nat. Rev. Mol. Cell Biol. 3, 639–650. https://doi.org/10.1038/nrm908.
Poels, J., Verlinden, H., Fichna, J., Van Loy, T., Franssens, V., Studzian, K., Janecka, A., Nachman, R.J., Vanden Broeck, J., 2007. Functional comparison of two evolutionary conserved insect neurokinin-like receptors. Peptides 28, 103–108. https://doi.org/10.1016/j.peptides.2006.06.014.
Poels, J., Birse, R.T., Nachman, R.J., Fichna, J., Janecka, A., Vanden Broeck, J., Nässel, D.R., 2009. Characterization and distribution of NKD, a receptor for *Drosophila* tachykinin-related peptide 6. Peptides 30, 545–556. https://doi.org/10.1016/j.peptides.2008.10.012.
Poels, J., Van Loy, T., Vandersmissen, H.P., Van Hiel, B., Van Soest, S., Nachman, R.J., Vanden Broeck, J., 2010. Myoinhibiting peptides are the ancestral ligands of the promiscuous *Drosophila* sex peptide receptor. Cell. Mol. Life Sci. 67, 3511–3522. https://doi.org/10.1007/s00018-010-0393-8.
Reagan, J.D., 1995. Functional expression of a diuretic hormone receptor in baculovirus-infected insect cells: evidence suggesting that the N-terminal region of diuretic hormone is associated with receptor activation. Insect Biochem. Mol. Biol. 25, 535–539. https://doi.org/10.1016/0965-1748(95)00021-4.
Reagan, J.D., 1996. Molecular cloning and function expression of a diuretic hormone receptor from the house cricket, *Acheta domesticus*. Insect Biochem. Mol. Biol. 26, 1–6. https://doi.org/10.1016/0965-1748(95)00074-7.
Rives, M.L., Rossillo, M., Liu-Chen, L.-Y., Javitch, J.A., 2012. 6'-Guanidinonaltrindole (6'-GNTI) is a G protein-biased κ-opioid receptor agonist that inhibits arrestin recruitment. J. Biol. Chem. 287, 27050–270504. https://doi.org/10.1074/jbc.C112.387332.
Saulière, A., Bellot, M., Paris, H., Denis, C., Finana, F., Hansen, J.T., Altié, M.-F., Seguelas, M.-H., Pathak, A., Hansen, J.L., Sénard, J.-M., Galés, C., 2012. Deciphering biased-agonism complexity reveals a new active AT1 receptor entity. Nat. Chem. Biol. 8, 622–630. https://doi.org/10.1038/nchembio.961.
Schiöth, H.B., Lagerström, M.C., 2008. Structural diversity of g proteincoupled receptors and significance for drug discovery. Nat. Rev. Drug Discov. 7, 339–357. https://doi.org/10.1038/nrd2518.
Schmitz, A.-L., Schrage, R., Gaffal, E., Charpentier, T.H., Wiest, J., Hiltensperger, G., Morschel, J., Hennen, S., Häußler, D., Horn, V., Wenzel, D., Grundmann, M., Büllesbach, K.M., Schröder, R., Brewitz, H.H., Schmidt, J., Gomeza, J., Galés, C., Fleischmann, B.K., Tüting, T., Imhof, D., Tietze, D., Gütschow, M., Holzgrabe, U., Sondek, J., Harden, T.K., Mohr, K., Kostenis, E., 2014. A cell-permeable inhibitor to trap $G\alpha_q$ proteins in the empty pocket conformation. Chem. Biol. 21, 890–902. https://doi.org/10.1016/J.CHEMBIOL.2014.06.003.
Schrage, R., Schmitz, A.L., Gaffal, E., Annala, S., Kehraus, S., Wenzel, D., Büllesbach, K.M., Bald, T., Inoue, A., Shinjo, Y., Galandrin, S., Shridhar, N., Hesse, M., Grundmann, M., Merten, N., Charpentier, T.H., Martz, M., Butcher, A.J., Slodczyk, T., Armando, S., Effern, M., Namkung, Y., Jenkins, L., Horn, V., Stößel, A., Dargatz, H., Tietze, D., Imhof, D., Gales, C., Drewke, C., Müller, C.E., Hölzel, M., Milligan, G., Tobin, A.B., Gomeza, J., Dohlman, H.G., Sondek, J., Harden, T.K., Bouvier, M., Laporte, S.A., Aoki, J., Fleischmann, B.K., Mohr, K., König, G.M., Tüting, T., Kostenis, E., 2015. The experimental power of FR900359 to study G_q-regulated biological processes. Nat. Commun. 6, 1–7. https://doi.org/10.1038/ncomms10156.
Sonnhammer, E.L., von Heijne, G., Krogh, A., 1998. A hidden Markov model for predicting transmembrane helices in protein sequences. Proc. Int. Conf. Intell. Syst. Mol.

Biol. 6, 175–182.
Te Brugge, V.A., Orchard, I., 2002. Evidence for CRF-like and kinin-like peptides as neurohormones in the blood-feeding bug, *Rhodnius prolixus*. Peptides 23, 1967–1979. https://doi.org/10.1016/S0196-9781(02)00184-5.
Te Brugge, V., Paluzzi, J.-P., Schooley, D. a, Orchard, I., 2011. Identification of the elusive peptidergic diuretic hormone in the blood-feeding bug *Rhodnius prolixus*: a CRF-related peptide. J. Exp. Biol. 214, 371–381. https://doi.org/10.1242/jeb.046292.
Tobe, S., Pratt, G., 1975. Corpus allatum activity *in vitro* during ovarian maturation in the desert locust, *Schistocerca gregaria*. J. Exp. Biol. 62, 611–627.
Tobe, S.S., Zhang, J.R., Schooley, D.A., Coast, G.M., 2005. A study of signal transduction for the two diuretic peptides of *Diploptera punctata*. Peptides 26, 89–98. https://doi.org/10.1016/j.peptides.2004.07.013.
Van Hiel, M.B., Van Wielendaele, P., Temmerman, L., Van Soest, S., Vuerinckx, K., Huybrechts, R., Vanden Broeck, J., Simonet, G., 2009. Identification and validation of housekeeping genes in brains of the desert locust *Schistocerca gregaria* under different developmental conditions. BMC Mol. Biol. 10, 56. https://doi.org/10.1186/1471-2199-10-56.
Van Wielendaele, P., Dillen, S., Marchal, E., Badisco, L., Vanden Broeck, J., 2012. CRF-like diuretic hormone negatively affects both feeding and reproduction in the desert locust, *Schistocerca gregaria*. PloS One 7, e31425. https://doi.org/10.1371/journal.pone.0031425.
Vandersmissen, H.P., Nachman, R.J., Vanden Broeck, J., 2013. Sex peptides and MIPs can activate the same G protein-coupled receptor. Gen. Comp. Endocrinol. 188, 137–143. https://doi.org/10.1016/j.ygcen.2013.02.014.
Vandesompele, J., De Preter, K., Pattyn, F., Poppe, B., Van Roy, N., De Paepe, A., Speleman, F., 2002. Accurate normalization of real-time quantitative RT-PCR data by geometric averaging of multiple internal control genes. Genome Biol. 3https://doi.org/10.1186/gb-2002-3-7-research0034. research0034.1.
Verlinden, H., Lismont, E., Bil, M., Urlacher, E., Mercer, A., Vanden Broeck, J., Huybrechts, R., 2013. Characterisation of a functional allatotropin receptor in the bumblebee, *Bombus terrestris* (Hymenoptera, Apidae). Gen. Comp. Endocrinol. 193, 193–200.
Verlinden, H., Vleugels, R., Verdonck, R., Urlacher, E., Vanden Broeck, J., Mercer, A., 2015. Pharmacological and signalling properties of a D2-like dopamine receptor (Dop3) in *Tribolium castaneum*. Insect Biochem. Mol. Biol. 56, 9–20. https://doi.org/10.1016/j.ibmb.2014.11.002.
Verlinden, H, Vleugels, R, Zels, S, Dillen, S, Lenaerts, C, Crabbé, K, Spit, J, Vanden Broeck, J, 2014. Receptors for neuronal and endocrine signalling molecules as potential targets for the control of insect pests. Adv. in Insect Phys. 46, 167–303. https://doi.org/10.1016/j.ibmb.2014.11.002.
Vleugels, R., Lenaerts, C., Baumann, A., Vanden Broeck, J., Verlinden, H., 2013. Pharmacological characterization of a 5-HT1-type serotonin receptor in the red flour beetle, *Tribolium castaneum*. PloS One 8, e65052. https://doi.org/10.1371/journal.pone.0065052.
Vuerinckx, K., Verlinden, H., Lindemans, M., Vanden Broeck, J., Huybrechts, R., 2011. Characterization of an allatotropin-like peptide receptor in the red flour beetle, *Tribolium castaneum*. Insect Biochem. Mol. Biol. 41, 815–822. https://doi.org/10.1016/j.ibmb.2011.06.003.
Yeoh, J.G.C., Pandit, A.A., Zandawala, M., Dick, R.N., Davies, S., Dow, J.A.T., 2017. DINeR : database for insect neuropeptide research. Insect Biochem. Mol. Biol. 86, 9–19. https://doi.org/10.1016/j.ibmb.2017.05.001.
Zels, S., Verlinden, H., Dillen, S., Vleugels, R., Nachman, R.J., Vanden Broeck, J., 2014. Signaling properties and pharmacological analysis of two Sulfakinin receptors from the red flour beetle, *Tribolium castaneum*. PloS One 9, e94502. https://doi.org/10.1371/journal.pone.0094502.